

1 **Estimating the atmospheric concentration of Criegee**  
2 **intermediates and their possible interference in a FAGE-LIF**  
3 **instrument**

4 Anna Novelli<sup>1,2</sup>, Korbinian Hens<sup>1</sup>, Cheryl Tatum Ernest<sup>1,3</sup>, Monica Martinez<sup>1</sup>, Anke C.  
5 Nölscher<sup>1,4</sup>, Vinayak Sinha<sup>5</sup>, Pauli Paasonen<sup>6</sup>, Tuukka Petäjä<sup>6</sup>, Mikko Sipilä<sup>6</sup>, Thomas Elste<sup>7</sup>,  
6 Christian Plass-Dülmer<sup>7</sup>, Gavin J. Phillips<sup>1,8</sup>, Dagmar Kubistin<sup>1,7,9</sup>, Jonathan Williams<sup>1</sup>, Luc  
7 Vereecken<sup>1,2</sup>, Jos Lelieveld<sup>1</sup> and Hartwig Harder<sup>1</sup>

8

9 [1] {Atmospheric Chemistry Department, Max Planck Institute for Chemistry, 55128 Mainz,  
10 Germany}

11 [2] Now at: {Institute of Energy and Climate Research, IEK-8: Troposphere,  
12 Forschungszentrum Jülich GmbH, 52428 Jülich, Germany}

13 [3] Now at: {Department of Neurology University Medical Center of the Johannes Gutenberg  
14 University Mainz, 55131 Mainz}

15 [4] Now at: {Division of Geological and Planetary Sciences, California Institute of  
16 Technology, Pasadena, USA}

17 [5] {Department of Earth and Environmental Sciences, Indian Institute of Science Education  
18 and Research Mohali, Sector 81 S.A.S. Nagar, Manauli PO, Mohali 140 306, Punjab, India}

19 [6] {Department of Physics., P.O. Box 64. 00014 University of Helsinki, Finland}

20 [7] {German Meteorological Service, Meteorological Observatory Hohenpeissenberg  
21 (MOHp), 83282 Hohenpeissenberg, Germany}

22 [8]{Department of Natural Sciences, University of Chester, Thornton Science Park, Chester,  
23 CH2 4NU, UK}

24 [9] {University of Wollongong, School of Chemistry, Wollongong, Australia}

25

1 Correspondence to: H. Harder (hartwig.harder@mpic.de)

## 2 **Abstract**

3 We analysed the extensive dataset from the HUMPPA-COPEC 2010 and the HOPE 2012  
4 field campaigns in the boreal forest and rural environments of Finland and Germany,  
5 respectively, and estimated the abundance of stabilised Criegee intermediates (SCI) in the  
6 lower troposphere. Based on laboratory tests, we propose that the background OH signal  
7 observed in our IPI-LIF-FAGE instrument during the afore-mentioned campaigns is caused at  
8 least partially by SCI. This hypothesis is based on observed correlations with temperature and  
9 with concentrations of unsaturated volatile organic compounds and ozone. Just like SCI, the  
10 background OH concentration can be removed through the addition of sulfur dioxide. SCI  
11 also adds to the previously underestimated production rate of sulfuric acid. An average  
12 estimate of the SCI concentration of  $\sim 5.0 \times 10^4$  molecules  $\text{cm}^{-3}$  (with an order of magnitude  
13 uncertainty) is calculated for the two environments. This implies a very low ambient  
14 concentration of SCI, though, over the boreal forest, significant for the conversion of  $\text{SO}_2$   
15 into  $\text{H}_2\text{SO}_4$ . The large uncertainties in these calculations, owing to the many unknowns in the  
16 chemistry of Criegee intermediates, emphasise the need to better understand these processes  
17 and their potential effect on the self-cleaning capacity of the atmosphere.

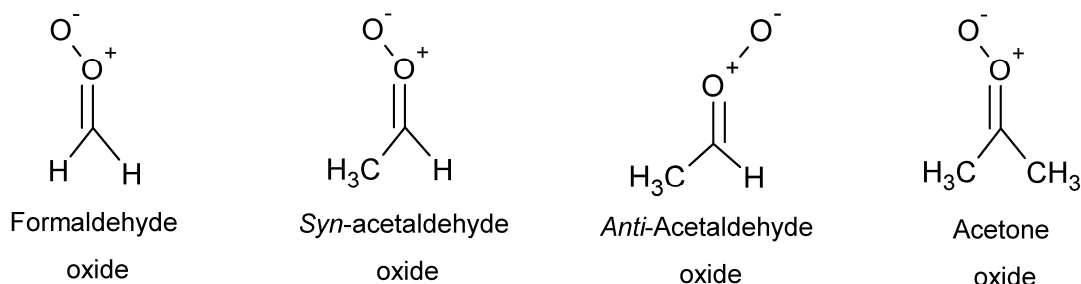
18

## 19 **1 Introduction**

20 Criegee intermediates (CI), or carbonyl oxides, are formed during the ozonolysis of  
21 unsaturated organic compounds (Criegee, 1975; Johnson and Marston, 2008; Donahue et al.,  
22 2011): in the gas phase ozone attaches to a double bond forming a primary ozonide (POZ)  
23 that quickly decomposes forming a Criegee intermediate and a carbonyl compound. The CI

1 can exist as thermally stabilised CI (SCI) or as chemically activated CI (Kroll et al.,  
 2 2001;Drozd et al., 2011), where the chemically activated CI have high energy content and in  
 3 the atmosphere either undergo unimolecular decomposition, or are stabilised by collisional  
 4 energy loss forming SCI.

5 For many decades the chemistry of Criegee intermediates was investigated both with  
 6 theoretical and indirect experimental studies as reviewed in detail by Johnson and Marston  
 7 (2008), Vereecken and Francisco (2012), and Vereecken et al. (2015). During the last few  
 8 years, numerous experimental studies specifically on stabilised Criegee intermediates have  
 9 been performed following their first detection by Welz et al. (2012). Many laboratories have  
 10 now detected SCI with various techniques (Berndt et al., 2012;Mauldin III et al.,  
 11 2012;Ouyang et al., 2013;Taatjes et al., 2013;Ahrens et al., 2014;Buras et al., 2014;Liu et al.,  
 12 2014a;Sheps et al., 2014;Novelli et al., 2014b;Stone et al., 2014;Chhantyal-Pun et al.,  
 13 2015;Lee, 2015;Newland et al., 2015a;Fang et al., 2016a;Smith et al., 2016) and have  
 14 confirmed that they are very reactive towards many atmospheric trace gases. Currently, the  
 15 most studied Criegee intermediates are formaldehyde oxide,  $\text{CH}_2\text{OO}$ , acetaldehyde oxide,  
 16  $\text{CH}_3\text{CHOO}$  (*syn* and *anti*, i.e. with the outer oxygen pointing towards or away from an alkyl  
 17 group, respectively) and acetone oxide,  $(\text{CH}_3)_2\text{COO}$ .



18

19 The importance of stabilised Criegee intermediates as oxidants in the atmosphere depends on  
 20 the rate coefficient of their reaction with water vapour as the latter is ubiquitously present in

1 relatively high concentrations in the boundary layer (between  $10^{16}$  to  $10^{17}$  molecules  $\text{cm}^{-3}$ ).  
2 The rate of this reaction strongly depends on the CI conformation (Aplincourt and Ruiz-  
3 López, 2000; Tobias and Ziemann, 2001; Ryzhkov and Ariya, 2003; Kuwata et al.,  
4 2010; Anglada et al., 2011; Anglada and Sole, 2016; Chen et al., 2016; Lin et al., 2016; Long et  
5 al., 2016) and until now the rate coefficient has been measured for *anti*-CH<sub>3</sub>CHOO (Taatjes  
6 et al., 2013; Sheps et al., 2014) while lower limits have been determined for CH<sub>2</sub>OO (Stone et  
7 al., 2014), *syn*-CH<sub>3</sub>CHOO (Taatjes et al., 2013; Sheps et al., 2014) and (CH<sub>3</sub>)<sub>2</sub>COO (Huang et  
8 al., 2015; Newland et al., 2015b). The uncertainties in these rate coefficients make it difficult  
9 to estimate the importance of Criegee intermediates and the impact they may have as oxidants  
10 in the atmosphere. Additionally, recent studies (Berndt et al., 2014b; Chao et al., 2015; Lewis  
11 et al., 2015; Smith et al., 2015; Lin et al., 2016) showed that the reaction between CH<sub>2</sub>OO and  
12 water dimers (present in the ppmv range in the atmosphere (Shillings et al., 2011)) is faster  
13 than the reaction with water vapor, in agreement with the several theoretical studies  
14 (Ryzhkov and Ariya, 2004; Chen et al., 2016; Lin et al., 2016) which indicate the reaction with  
15 water dimers to be between 400 and 35,000 times faster than the reaction with water vapor  
16 depending on the conformers. Another important reaction of SCI that depends on the SCI  
17 conformation is their unimolecular decomposition. The decomposition rate and product  
18 formed depend on the SCI conformer structure. *Anti*-SCI are likely to isomerise via the ester  
19 channel forming an ester or an acid as final product while *syn*-SCI will form a vinyl  
20 hydroperoxide (VHP) which promptly decomposes forming hydroxyl radicals (OH) and a  
21 vinoxy radical (Paulson et al., 1999; Johnson and Marston, 2008; Drozd and Donahue,  
22 2011; Vereecken and Francisco, 2012; Kidwell et al., 2016). Larger and more complex  
23 conformers such as hetero-substituted or cyclic structures are subject to additional  
24 unimolecular rearrangements (Vereecken and Francisco, 2012). On the unimolecular

1 decomposition rates and products few experimental data are available (Horie et al.,  
2 1997;Horie et al., 1999;Fenske et al., 2000a;Novelli et al., 2014b;Kidwell et al., 2016;Fang et  
3 al., 2016a;Smith et al., 2016), but more is available from theoretical studies explicitly  
4 focusing on the path followed by different conformers (Anglada et al., 1996;Aplincourt and  
5 Ruiz-López, 2000;Kroll et al., 2001;Zhang and Zhang, 2002;Nguyen et al., 2009b;Kuwata et  
6 al., 2010).

7 Most of the experimental and theoretical information described above refers to the smaller  
8 conformers. These compounds are likely to be formed relatively efficiently in the atmosphere  
9 as they can originate from any unsaturated compound with a terminal double bond, but they  
10 do not represent the entire Criegee intermediate population.

11 As SCI were found to react quickly with many trace gases, various model studies were  
12 performed on the impact SCI have as oxidants in the atmosphere (Vereecken et al., 2012;Boy  
13 et al., 2013;Percival et al., 2013;Pierce et al., 2013;Sarwar et al., 2013;Sarwar et al.,  
14 2014;Novelli et al., 2014b;Vereecken et al., 2014). Some of these studies focused in  
15 particular on the possible impact that SCI might have on the formation of sulfuric acid  
16 ( $\text{H}_2\text{SO}_4$ ) in the gas phase, following Mauldin III et al. (2012) who suggested that Criegee  
17 intermediates are the missing  $\text{SO}_2$  oxidant needed to close the sulfuric acid budget over a  
18 boreal forest. This is supported by theoretical and laboratory studies that have determined a  
19 rate coefficient between SCI and sulfur dioxide ( $\text{SO}_2$ ) of the order of  $10^{-11} \text{ cm}^3 \text{ molecule}^{-1} \text{ s}^{-1}$   
20 (Aplincourt and Ruiz-López, 2000;Jiang et al., 2010;Kurtén et al., 2011;Vereecken et al.,  
21 2012;Welz et al., 2012;Taatjes et al., 2013;Liu et al., 2014b;Sheps et al., 2014;Stone et al.,  
22 2014). As the main atmospherically relevant oxidiser of  $\text{SO}_2$  in the gas phase is the OH  
23 radical with a rather slow rate coefficient at ambient temperature and pressure of  $2 \times 10^{-12}$   
24  $\text{cm}^3 \text{ molecule}^{-1} \text{ s}^{-1}$  (Atkinson et al., 2004), the high rate coefficient for  $\text{SO}_2$  oxidation would

1 allow SCI to have a significant impact on the  $\text{H}_2\text{SO}_4$  formation even if present in small  
2 concentrations. The model studies have shown that, depending on the environment, SCI can  
3 have a potentially important impact on  $\text{H}_2\text{SO}_4$  formation. All these studies are affected by  
4 large uncertainties and many simplifications used for coping with the paucity of data on the  
5 reactions of specific SCI with various trace gas species, on the speciation of SCI, and on the  
6 steady state concentration of SCI in the troposphere. Until now no direct or reproducible  
7 indirect method was able to determine the steady state concentration of SCI in the lower  
8 troposphere.

9 In this paper, we firstly estimate the concentration of SCI in the lower troposphere, based on  
10 the data collected during the HUMPPA-COPEC 2010 campaign (Williams et al., 2011) in a  
11 Boreal forest in Finland and the HOPE 2012 campaign in rural southern Germany. The  
12 budget of SCI is analyzed using four different approaches: 1) based on an unexplained  $\text{H}_2\text{SO}_4$   
13 production rate (Mauldin III et al., 2012); 2) from the measured concentrations of unsaturated  
14 volatile organic compounds (VOC); 3) from the observed OH reactivity (Nölscher et al.,  
15 2012); and 4) from an unexplained production rate of OH (Hens et al., 2014). Secondly, we  
16 present measurements obtained using our inlet pre-injector laser-induced fluorescence assay  
17 by gas expansion technique (IPI-LIF-FAGE) (Novelli et al., 2014a) during the HUMPPA-  
18 COPEC 2010 and the HOPE 2012 campaigns. A recent laboratory study performed with the  
19 same instrumental setup showed that the IPI-LIF-FAGE system is sensitive to the detection  
20 of the OH formed from unimolecular decomposition of SCI (Novelli et al., 2014b). Building  
21 on this study, the background OH ( $\text{OH}_{\text{bg}}$ ) (Novelli et al., 2014a) measured during the two  
22 field campaigns is investigated in comparison with many other trace gases in order to assess  
23 if the observations in controlled conditions are transferable to the ambient conditions.

24

## 2 Instrumentation and field sites

### 2.1 IPI-LIF-FAGE description

A comprehensive description of the IPI-LIF-FAGE ground-based instrument, HORUS (Hydroxyl Radical Measurement Unit based on fluorescence Spectroscopy), is given by Novelli et al. (2014a) and only some important features of the instrument are highlighted here. The IPI-LIF-FAGE instrument consists of: the inlet pre-injector (IPI), the inlet and detection system, the laser system, the vacuum system and the instrument control and data acquisition unit. The air is drawn through a critical orifice into a low pressure region ( $\sim 300$ - $500$  Pa) where OH molecules are selectively excited by pulsed UV light around 308 nm. The light is generated at a pulse repetition frequency of 3 kHz by a Nd:YAG pumped, pulsed, tunable dye laser system and is directed into a multipass "White cell" making 32 passes through the detection volume (White, 1942). The air sample intersects the laser beam and the fluorescence signal from the excited OH molecules is detected using a gated micro-channel plate (MCP) detector. IPI, situated in front of the instrument inlet, is used to measure a chemical zero to correct for possible internal OH signal generation. An OH scavenger (propene) is added to the sample air 5 cm in front of the inlet pinhole in a concentration that allows a known, high proportion of atmospheric OH to be scavenged ( $\sim 90$  %). The OH scavenger is added every two minutes so that the instrument measures a total OH signal ( $\text{OH}_{\text{tot}}$ ) when the OH scavenger is not injected and a background OH signal ( $\text{OH}_{\text{bg}}$ ) when the OH scavenger is injected. The difference between these two signals yields the atmospheric OH concentration ( $\text{OH}_{\text{atm}}$ ). The efficiency of this technique for measuring OH with this particular LIF-FAGE instrument is described together with the IPI characterisation in Novelli et al. (2014a). The OH calibration of the HORUS instrument is obtained via the production of

1 a known amount of OH and hydroperoxyl radicals ( $\text{HO}_2$ ) from the photolysis of water at 185  
2 nm using a mercury lamp. A more detailed description of the instrument calibration is  
3 reported by Martinez et al. (2010) and Hens et al. (2014). A calibration factor for the  
4 background OH signal observed by the HORUS instrument is currently not available.  
5 Therefore, this signal will be discussed and plotted in OH fluorescence counts per seconds  
6 (cps) measured by the MCP, normalized by the laser power and corrected for quenching and  
7 sensitivity changes towards the detection of OH. The sensitivity of the instrument towards the  
8 OH radical is affected by: alignment of the white cell, optical transmission of the  
9 components, sensitivity of the MCP, water vapor, internal pressure, and internal temperature  
10 (Martinez et al., 2010). These factors affect the sensitivity of HORUS towards the  
11 background OH in a similar manner as they mainly impact the sensitivity of the instrument to  
12 the detection of OH.

13 We hypothesise that the  $\text{OH}_{\text{bg}}$  is formed chemically within the IPI-LIF-FAGE instrument.  
14 Laser induced production of OH radicals was thoroughly tested in the laboratory and in the  
15 field (Novelli et al., 2014a) showing that this background OH signal is not induced by the  
16 laser beam from double pulsing, nor from air stagnating in the detection cell. By changing the  
17 laser power, no quadratic dependency of the  $\text{OH}_{\text{bg}}$  was observed even at night time, when the  
18 contribution of the  $\text{OH}_{\text{bg}}$  to the  $\text{OH}_{\text{tot}}$  measured by the instrument is highest (Novelli et al.,  
19 2014a). In addition, during the HUMPPA-COPEC 2010 and HOPE 2012 campaigns, the  
20 correlation coefficient of the  $\text{OH}_{\text{bg}}$  with the laser power was  $R = 0.002$  and  $R = 0.2$ ,  
21 respectively.

22 In contrast, ozonolysis of alkenes performed during laboratory tests showed that the IPI-LIF-  
23 FAGE instrument is sensitive to the OH formed from unimolecular decomposition of SCI  
24 within the low pressure section of the instrument (Novelli et al., 2014b).



1 Recently, most of the LIF-FAGE instruments have been augmented with the titration of  
2 OH<sub>atm</sub> in different environments to determine their background (Amédro, 2012;Mao et al.,  
3 2012;Griffith et al., 2013;Woodward-Massey et al., 2015;Griffith et al., 2016;Tan et al.,  
4 2016). Some of these instruments showed the presence of an unknown interference (Mao et  
5 al., 2012;Griffith et al., 2013;Tan et al., 2016) while for others no clear conclusions were  
6 drawn (Amédro, 2012;Woodward-Massey et al., 2015). In addition, laboratory studies (Fuchs  
7 et al., 2016;Griffith et al., 2016) have shown similarity with what was observed with the IPI-  
8 LIF-FAGE during experiments of ozonolysis of alkenes although the origin of the OH signal  
9 was not uniquely attributed to a particular mechanism.

10 Our hypothesis is that the OH<sub>bg</sub> measured in ambient air with the IPI-LIF-FAGE at least  
11 partially originates from unimolecular decomposition of SCI. Section 4 describes the  
12 observed behaviour of the signal during the campaigns and its relationship to other observed  
13 chemical tracers and discusses if this is compatible with our hypothesis.

## 15 **2.2 Measurement site and ancillary instrumentation**

16 We present measurements from two sites, a boreal forest site in Finland and a rural site in  
17 Southern Germany. The HUMPPA-COPEC 2010 (Hyytiälä United Measurements of  
18 Photochemistry and Particles in Air – Comprehensive Organic Precursor Emission and  
19 Concentration study) campaign took place during summer 2010 at the SMEAR II station in  
20 Hyytiälä, Finland (61° 51' N, 24°17' E, 181 m a.s.l.) in a boreal forest dominated by Scots  
21 Pines (*Pinus Silvestris L.*). The site hosts continuous measurements of several trace gases and  
22 meteorological parameters as well as aerosol particles concentrations, size distributions and  
23 composition (Junninen et al., 2009). Further details and a more complete description of the

1 site, the instrumentation and the meteorological conditions during the campaign can be found  
2 in Williams et al. (2011) and Hens et al. (2014). A brief description of the instruments used in  
3 this study is given here. Ozone was measured by a UV photometric gas analyser (Model 49,  
4 Thermo Electron Corporation). A gas chromatograph (GC, Agilent Technologies 6890A)  
5 coupled to a mass-selective detector (MS, Agilent Technologies MSD 5973 *inert*) was used  
6 for the measurements of biogenic volatile organic compounds (BVOC) (Yassaa et al., 2012).  
7 The total OH reactivity was measured by the comparative reactivity method (CRM) (Sinha et  
8 al., 2008) for two different heights, one within and one above the canopy (18 and 24 m,  
9 respectively) (Nölscher et al., 2012). CRM uses an in-situ kinetics experiment to measure the  
10 OH reactivity based on the competitive scavenging of OH by a reference gas (pyrrole) and  
11 atmospheric OH reactants. The overall uncertainty of the method during deployment was  
12 16% with a limit of detection of  $3.0 \text{ s}^{-1}$  (Hens et al., 2014). Sulfur dioxide ( $\text{SO}_2$ )  
13 concentration was measured with a fluorescence analyzer (Model 43S, Thermo 20  
14 Environmental Instruments Inc.). Aerosol number size distributions between 3.0 nm and 950  
15 nm were measured with a Differential Mobility Particle Sizer (DMPS) (Aalto et al., 2001).  
16 The size distributions were used for calculating the loss rate of gas-phase sulfuric acid via  
17 condensation sink (CS) with the method presented by Kulmala et al. (2001). Sulfuric acid  
18 ( $\text{H}_2\text{SO}_4$ ) and OH radical concentrations were measured on the ground with a chemical  
19 ionization mass spectrometer (CIMS; (Petäjä et al., 2009)). Time series of the measured trace  
20 gases are available in the study from Nölscher et al. (2012) and Hens et al. (2014). The  
21 average concentrations and their  $1\sigma$  variability are listed in Table 1 and Table SI-2. For the  
22 first period of the campaign, between the 27<sup>th</sup> and the 31<sup>st</sup> of July, the IPI-LIF-FAGE  
23 instrument was run on the ground side-by-side with the CIMS. On the 2<sup>nd</sup> of August the IPI-  
24 LIF-FAGE instrument was moved to the top of the HUMPPA tower above the canopy and

1 measured there for the remainder of the campaign (12<sup>th</sup> of August). The data are therefore  
2 separated into ground and tower periods

3 The HOPE 2012 (Hohenpeißenberg Photochemistry Experiment) campaign was conducted  
4 during the summer of 2012 at the Meteorological Observatory in Hohenpeißenberg, Bavaria,  
5 Germany (47° 48' N, 11° 2' E). The observatory is a Global Atmosphere Watch (GAW)  
6 station operated by the German Meteorological Service (DWD) and is located at an altitude  
7 of 985 m a.s.l. and about 300 m above the surrounding terrain, mainly consisting of meadows  
8 and coniferous forests. More information about the site can be found in Handisides et al.  
9 (2003). Ozone was measured by UV absorption with TEI 49C (Thermo Electron Corporation,  
10 Environmental Instruments) (Gilge et al., 2010). Non-methane hydrocarbons (NMHC) were  
11 measured with a GC-flame ionization detection (FID) system (series 3600CX, Varian,  
12 Walnut Creek, CA, USA) (Plass-Dülmer et al., 2002). BVOC were detected using a GC  
13 (Agilent 6890) with a FID running in parallel with a MS (Agilent Technologies MSD 5975  
14 *inertXL*) described by Hoerger et al. (2014). Photolysis frequencies ( $J(\text{NO}_2)$  and  $J(\text{O}^1\text{D})$ ) were  
15 measured next to the IPI-LIF-FAGE with a set of filter radiometers (Handisides et al., 2003).  
16 The OH reactivity was measured with two instruments for a short period of time from the 10<sup>th</sup>  
17 until the 18<sup>th</sup> of July. One method was the CRM and the same instrument was used as during  
18 the HUMPPA-COPEC 2010 campaign. The second method was a new application of the  
19 DWD CIMS instrument (Berresheim et al., 2000) which also measured  $\text{H}_2\text{SO}_4$  and OH  
20 radicals. As the data will be used only in a qualitative way for the current study, a very short  
21 description of this novel technique is given here and details will be presented in a future  
22 publication. With the CIMS instrument, OH radicals are measured by converting them into  
23  $\text{H}_2\text{SO}_4$  after reaction with  $\text{SO}_2$  in a chemical reactor and subtraction of a corresponding  
24 background after scavenging the OH with propane (Berresheim et al, 2000). A second  $\text{SO}_2$

1 titration zone was used 15 cm (or 140 ms) downstream of the first injection to determine the  
 2 OH decay from OH radicals generated in the UV-calibration zone immediately upstream of  
 3 the first titration. The difference between these two titration zones in two consecutive 2.5 min  
 4 intervals allows the determination of the OH decay, after correcting for ambient OH and wall  
 5 losses. The uncertainty is estimated at  $\pm 2.0 \text{ s}^{-1}$  and the limit of detection is  $2.0 \text{ s}^{-1}$ .  $\text{SO}_2$   
 6 concentration was measured with a fluorescence analyzer and aerosol size distributions were  
 7 measured and used to calculate the loss rate of gas-phase sulfuric acid due to CS formed by  
 8 existing aerosol surface via the method presented by (Birmili et al., 2003). Time series of the  
 9 measured trace gases are available in Figure SI-1. The average concentrations and their  $1\sigma$   
 10 variability are listed in Table 1 and Table SI-2

11

### 12 **3 SCI concentrations during HUMPPA-COPEC 2010 and HOPE 2012**

#### 13 **3.1 Missing $\text{H}_2\text{SO}_4$ oxidant**

14 The study by Mauldin III et al. (2012) in a boreal forest during the HUMPPA-COPEC 2010  
 15 campaign showed a consistent discrepancy between the measured  $\text{H}_2\text{SO}_4$  and the calculated  
 16 gas phase  $\text{H}_2\text{SO}_4$  concentration when considering oxidation of  $\text{SO}_2$  from OH radical and the  
 17 condensation onto pre-existing aerosol particles (CS, condensation sink) as the sole  
 18 production and loss processes, respectively (Eq. 1).

$$19 \quad [\text{H}_2\text{SO}_4] = \frac{k_{\text{OH}+\text{SO}_2} \times [\text{OH}] \times [\text{SO}_2]}{\text{CS}} \quad (1)$$

20 The  $\text{H}_2\text{SO}_4$  concentration is assumed to be in near-steady state: the lifetime of  $\text{H}_2\text{SO}_4$  in the  
 21 gas phase is of the order of minutes, i.e. spanning a similar time period compared to the  
 22 variability in the production and loss pathways, ensuring fast response of the  $\text{H}_2\text{SO}_4$

concentration to varying conditions. Minor deviations from steady state are not critical for the analysis performed in this study, given the uncertainties induced by other parameters.

On average the sulfuric acid in the gas phase calculated using Eq. 1 was only half of the total  $H_2SO_4$  observed in the field and lied outside the uncertainties associated with the calculation of the formation channel and the condensation sink (Mauldin III et al., 2012). Although no unambiguous evidence links SCI to the missing oxidant, laboratory tests performed with a similar instrument (Berndt et al., 2012; Berndt et al., 2014a; Sipilä et al., 2014) confirmed the role that SCI could have in the oxidation of  $SO_2$  and formation of  $H_2SO_4$ . Assuming that SCI are the only other species in addition to OH that oxidize  $SO_2$  in the gas phase and knowing the rate coefficient of SCI and OH with  $SO_2$ , it is possible to calculate the steady state concentration of SCI in that environment:

$$[H_2SO_4] = \frac{(k_{OH+SO_2} \times [OH] + k_{SCI+SO_2} \times [SCI]) \times [SO_2]}{CS} \quad (2)$$

The rate coefficient between OH and  $SO_2$  at standard pressure is  $(2.0 \pm 0.1) \times 10^{-12} (T/300)^{-0.27} \text{ cm}^3 \text{ molecule}^{-1} \text{ s}^{-1}$  (Atkinson et al., 2004). The rate coefficient of SCI with  $SO_2$  was determined by several groups at  $(3.3 \pm 2.0) \times 10^{-11} \text{ cm}^3 \text{ molecule}^{-1} \text{ s}^{-1}$ , (Welz et al., 2012; Taatjes et al., 2013; Liu et al., 2014b; Sheps et al., 2014; Stone et al., 2014; Chhantyal-Pun et al., 2015; Newland et al., 2015a; Newland et al., 2015b; Foreman et al., 2016; Zhu et al., 2016). An earlier, lower value of  $\sim 5.0 \times 10^{-13} \text{ cm}^3 \text{ molecule}^{-1} \text{ s}^{-1}$  (Mauldin III et al. (2012); Berndt et al. (2012)) appears to be hard to reconcile with the remaining literature, as extensively discussed in the supporting information.

Equation 2 allows for the calculation of a time series of SCI (Fig. SI-2) yielding an average  $[SCI] = (2.3 \pm 2.0) \times 10^4 \text{ molecules cm}^{-3}$ . A similar estimate of the SCI time series was derived for the HOPE 2012 campaign (Fig. SI-3). These time series are discussed in more

1 details in the supporting information; for the estimation of atmospheric SCI here we focus  
2 mostly on the overall concentration.

3 The  $\text{H}_2\text{SO}_4$  concentration during this campaign can be mainly explained by the reaction  
4 between OH and  $\text{SO}_2$ . Figure 1 shows the correlation between the total production rate of  
5  $\text{H}_2\text{SO}_4$  ( $P(\text{H}_2\text{SO}_4)_{\text{tot}}$ ) calculated from the product of measured  $\text{H}_2\text{SO}_4$  and the condensation  
6 sink, as well as the production rate of  $\text{H}_2\text{SO}_4$  from the reaction of OH and  $\text{SO}_2$ . The linear  
7 regression following the method of York et al. (2004) yields a slope of  $0.9 \pm 0.02$  with a  
8 negligible intercept ( $57 \pm 7.0 \text{ molecules cm}^{-3} \text{ s}^{-1}$ ). It should be noted that the  $\text{H}_2\text{SO}_4$  budget  
9 for the HOPE 2012 campaign is nearly closed, such that the moderate fluctuations on the  
10 source data (CS, [OH], etc.) lead to very large relative uncertainties of the small missing  
11  $\text{H}_2\text{SO}_4$  production term, and concomitantly the time series for the SCI concentration (Fig. SI-  
12 3) shows extreme variability reflecting this noise on the source data. On average, the [SCI]  
13 obtained is low,  $(2.0 \pm 3.0) \times 10^4 \text{ molecules cm}^{-3}$ , with no values in the time series exceeding  
14  $10^5 \text{ molecule cm}^{-3}$ .

15 Repeating the above analysis using the low  $k_{\text{SCI}+\text{SO}_2}$  value of Mauldin III et al. and Berndt et  
16 al. yields concentrations of  $(1.6 \pm 2.0) \times 10^6$  and  $(1.0 \pm 3.0) \times 10^6 \text{ molecule cm}^{-3}$  for the  
17 HUMPPA-COPEC and HOPE campaigns, respectively. It is interesting to notice that both  
18 values estimated with the fast and low  $k_{\text{SCI}+\text{SO}_2}$  rate coefficient are in agreement with the  
19 concentrations calculated from measured VOC and  $\text{O}_3$  for polluted and pristine environments,  
20  $1.9 \times 10^6 \text{ molecules cm}^{-3}$  and  $4.5 \times 10^4 \text{ molecules cm}^{-3}$  respectively, from a previous study  
21 (Welz et al., 2012).

22

## 3.2 Measured unsaturated VOC

Another method to estimate the SCI concentration is based on their production and loss processes. In a forest SCI are expected to be formed from the ozonolysis of unsaturated BVOC. It is possible to calculate an average steady state concentration for SCI using the following equation

$$[SCI] = \sum_i \left( \frac{k_{VOC_i+O_3} \times [VOC_i] \times Y_{SCI}}{L_{SCI_{syn}}} \right) \times [O_3] \quad (3)$$

Where  $k_{VOC_i+O_3}$  is the rate coefficient between the  $VOC_i$  and ozone (Table SI-2),  $Y_{SCI}$  is the yield of SCI in the ozonolysis reaction, and  $L_{SCI_{syn}}$  is the total loss of *syn*-SCI. We assume  $[SCI] \approx [SCI_{syn}]$  following the model described by Novelli et al. (2014b), which accounts for many possible losses of SCI including the reaction with water dimers and unimolecular decomposition. The latter study suggests that *anti*-acetaldehyde oxide and formaldehyde oxide react quickly with water and water dimers and that their contributions can be neglected. A yield of SCI formation ( $Y_{SCI}$ ) of 0.4 was estimated based on the data by Hasson et al. (2001). The steady state concentration of SCI for the HUMPPA-COPEC 2010 campaign was calculated using the measured data for  $[O_3]$  and  $[VOC_i]$  and an average value of  $40 \text{ s}^{-1}$  (Novelli et al., 2014b) for  $L_{SCI_{syn}}$  as this value was found to be rather constant and mainly dependent on the unimolecular decomposition rate of the SCI. Equation 3 allows for the calculation of a time series of SCI (Fig. SI-4) yielding an average  $[SCI]$  of  $\sim (5.0 \pm 4.0) \times 10^3 \text{ molecules cm}^{-3}$ . These time series are discussed in more details in the supporting information; for the estimation of atmospheric SCI here we focus mostly on the overall concentration. During the HOPE 2012 campaign a larger number of unsaturated organic trace gases, both anthropogenic and biogenic, were measured (Table SI-1). For  $Y_{SCI}$  the same value of 0.4 was

used while for  $L_{SCI_{syn}}$  the value of  $32 \text{ s}^{-1}$ , obtained from the model described by Novelli et al. (2014b) for the rural European environment, was used. Using these values in Eq. 3 results in  $[SCI] = (7.0 \pm 6.0) \times 10^3 \text{ molecules cm}^{-3}$ , obtained as an average of the SCI time series (Fig. SI-5). It should be noted that recent work on the unimolecular decomposition (Fang et al., 2016b; Long et al., 2016; Smith et al., 2016) yields loss rates significantly faster than used here; this implies that the  $[SCI]$  obtained here could be an overestimate.

### 3.3 OH reactivity

During HUMPPA-COPEC 2010, between 27<sup>th</sup> July and 12<sup>th</sup> August, an average OH reactivity,  $R = 9.0 \pm 7.6 \text{ s}^{-1}$ , was measured. On average, the majority of the measured OH reactivity ( $R_{unex} = 7.4 \pm 7.4 \text{ s}^{-1}$ , i.e. 80 %) was not accounted for by the measured organic and inorganic trace gases (Fig. SI-6). Biogenic emissions comprised up to ~ 10 % of the total measured OH reactivity and up to half of the calculated OH reactivity (Fig. SI-6). As the measurement site was located in a pristine forest environment, affected only little by anthropogenic emissions (Williams et al., 2011), it is likely that a large fraction of the unexplained OH reactivity was formed by unmeasured primary emissions by the vegetation and secondary products of oxidation. By assuming that the unmeasured VOC are unsaturated, and by using a lumped rate coefficient,  $k_{VOC+OH}$ , between OH and the fraction of unspciated VOC of  $7.0 \times 10^{-11} \text{ cm}^3 \text{ molecule}^{-1} \text{ s}^{-1}$ , typical for an OH addition to a carbon-carbon double bond (Atkinson et al., 2004; Peeters et al., 2007), it is possible to estimate the concentration  $[VOC_{unknown}]$  of VOC that would be necessary to close the OH reactivity budget (Eq. 4).

$$R_{unex} = k_{VOC+OH} \times [VOC_{unknown}] \quad (4)$$



1 Using Eq. 4, a time series for  $[VOC_{unknown}]$  with an average of  $(1.0 \pm 1.0) \times 10^{11}$  molecules  
2  $\text{cm}^{-3}$  is obtained. These values are substituted into Eq. 3 and a lumped rate coefficient  $k$  of  $7.0$   
3  $\times 10^{-17}$  molecules  $\text{cm}^{-3}$  is used for reaction of  $[VOC_{unknown}]_t$  with  $[O_3]_t$  at time  $t$ . This  $k$  value  
4 is based on the rate coefficient of the measured VOC with  $O_3$  weighted with their abundance  
5 (Table SI-1). The same  $Y_{SCI}$  and  $L_{SCI_{syn}}$  of 0.4 and  $40 \text{ s}^{-1}$ , respectively, were used as described  
6 in section 3.2. With these values, a time series of SCI (Fig. SI-7) with an average of  $\sim (1.0 \pm$   
7  $1.0) \times 10^5$  molecules  $\text{cm}^{-3}$  is obtained. To this SCI concentration estimate, we add the SCI  
8 formed from the measured unsaturated VOC,  $[SCI] = (5.0 \pm 4.0) \times 10^3$  molecules  $\text{cm}^{-3}$ , to  
9 obtain the total SCI across all VOC. As this estimate requires assumptions for the rate  
10 coefficient between  $[VOC_{unknown}]$  and OH and  $O_3$ , a sensitivity study probing the upper and  
11 lower bounds of this estimate is described in the supplementary information. The time series  
12 are discussed in more details in the supporting information; for the estimation of atmospheric  
13 SCI here we focus mostly on the overall concentration.

14 During the HOPE 2012 campaign the total OH reactivity was on average  $3.5 \pm 3.0 \text{ s}^{-1}$ . Using  
15 the measured trace gas concentrations it is possible to calculate the expected OH reactivity  
16 (Fig. SI-8). Table SI-2 lists all the species included in the calculation of the OH reactivity  
17 with their rate coefficient with OH. An average value of  $2.7 \pm 0.7 \text{ s}^{-1}$  was calculated. Figure  
18 SI-8 shows that half of the measured OH reactivity can be explained by methane, carbonyl  
19 compounds (mainly acetaldehyde and propanal) and inorganic compounds which were  
20 present in higher concentrations compared to the HUMPPA-COPEC 2010 campaign (Table  
21 SI-2). On average, 24 % of the measured OH reactivity remains unexplained by the measured  
22 trace gases. In contrast to the HUMPPA-COPEC 2010 campaign, in HOPE 2012 a more  
23 complete speciation of VOC was measured (Table SI-1) and the site was influenced by  
24 relatively fresh anthropogenic emissions. With the extensive VOC speciation available, the

1 reactivity budget can virtually be closed, but any remaining unexplained OH reactivity could  
2 still be due to unmeasured VOC. The time series for this unexplained OH reactivity, typically  
3 about  $\sim 1 \text{ s}^{-1}$ , shows very large variability as it reflects the statistical noise of the small  
4 difference between measured and calculated OH reactivities, both of which are associated  
5 with variability. The resulting [SCI] time series (Fig. SI-9) is also highly variable, and yields  
6 a low average SCI concentration of  $(2.0 \pm 1.5) \times 10^4 \text{ molecules cm}^{-3}$ , with no values  
7 exceeding  $6.0 \times 10^4 \text{ molecule cm}^{-3}$ .

8 The total SCI is then obtained by summing the SCI predicted from the measured VOC and  
9 from the unexplained OH reactivity, leading to a total SCI concentration of  $(7.0 \pm 6.0) \times 10^3$   
10 molecules  $\text{cm}^{-3}$ .

### 12 **3.4 Unexplained OH production rate**

13 During the HUMPPA-COPEC 2010 campaign, the comprehensive measurements (Williams  
14 et al., 2011) allowed the calculation of a detailed OH budget (Hens et al., 2014). Most of the  
15 OH production during daytime is due to photolysis of  $\text{O}_3$  and recycling of  $\text{HO}_2$  back to OH  
16 via reactions with NO and  $\text{O}_3$ . This result holds for both high ( $R > 15 \text{ s}^{-1}$ ) and low ( $R \leq 15 \text{ s}^{-1}$ )  
17 OH reactivity episodes during the campaign. While the OH budget can be closed during  
18 daytime ( $J(\text{O}^1\text{D}) > 3.0 \times 10^{-6} \text{ s}^{-1}$ ) for low OH reactivity periods, during periods with high OH  
19 reactivity there was a large unexplained production rate of OH,  $P_{\text{OH}}^{\text{unexplained}} = (2.0 \pm 0.7) \times 10^7$   
20 molecule  $\text{cm}^{-3} \text{ s}^{-1}$ , which can thus be surmised to originate from VOC chemistry. In addition,  
21 for both periods, during night time ( $J(\text{O}^1\text{D}) \leq 3.0 \times 10^{-6} \text{ s}^{-1}$ ), the IPI-LIF-FAGE and the CIMS  
22 instruments both measured non-negligible OH concentrations (Hens et al., 2014) where most

1 of the OH production was from unknown sources ( $P_{OH}^{unexplained} = 1.0 \pm 0.9 \times 10^6 \text{ molecule cm}^{-3}$   
 2  $\text{s}^{-1}$  ( $1\sigma$ ) and  $P_{OH}^{unexplained} = 1.7 \pm 0.7 \times 10^7 \text{ molecule cm}^{-3} \text{ s}^{-1}$  ( $1\sigma$ ) for low and high reactivity,  
 3 respectively). Our hypothesis is that ozonolysis of VOC could represent the missing OH  
 4 source. Indeed, formation of OH from oxidation of unsaturated VOC has been shown to be an  
 5 important source of OH in winter, indoors and during night time (Paulson and Orlando,  
 6 1996;Geyer et al., 2003;Ren et al., 2003;Heard et al., 2004;Harrison et al., 2006;Johnson and  
 7 Marston, 2008;Shallcross et al., 2014). As OH formation from ozonolysis proceeds through  
 8 Criegee intermediates (Fig. 2), we can attempt to estimate a SCI concentration from the OH  
 9 budget. First, we estimate from the unexplained OH production  $P_{OH}^{unexplained}$  a so-called  
 10 unexplained  $\text{O}_3$  reactivity,  $\Sigma(k_{\text{VOC}+\text{O}_3} \times [\text{VOC}_{\text{unidentified}}])$ , assuming a certain yield of OH from  
 11 ozonolysis of unsaturated VOC. Next, we estimate a yield of SCI based on available literature  
 12 data, and finally we combine both to estimate the SCI concentration required to close the OH  
 13 budget. In contrast to the previous estimates, an average value is obtained for the SCI, and  
 14 not a time series, as we start from the average  $P_{OH}^{unexplained}$ , as reported in Hens et al. (2014).  
 15 Assuming that all unexplained OH production,  $P_{OH}^{unexplained}$ , comes from VOC ozonolysis with  
 16 a certain OH yield  $Y_{OH}$  we obtain:

$$17 \quad P_{OH}^{unexplained} = k_{\text{voc}+\text{O}_3} \times [\text{VOC}_{\text{unidentified}}] \times [\text{O}_3] \times Y_{OH} \quad (5)$$

18 where  $\text{VOC}_{\text{unidentified}}$  includes the VOC not considered in the OH budget performed by Hens  
 19 et al. (2014), i.e. the VOC causing the unknown OH reactivity discussed above. The average  
 20 total OH yield from ozonolysis,  $Y_{OH}$ , is estimated at about 0.6 based on observed OH yields  
 21 from the literature (Atkinson et al., 2006). OH formation from ozonolysis occurs through two  
 22 channels (Fig. 2): prompt formation by the decomposition of chemically activated  $\text{CI}^*$ , and

1 delayed OH by formation of SCI followed by their thermal decomposition; there are also  
 2 product channels not yielding OH. The prompt yield of OH,  $Y_{OH}^{CI^*}$  is estimated at  $\sim 0.4$  from  
 3 SCI scavenging experiments (Atkinson et al., 2004); the remaining yield  $Y_{OH}^{SCI}$  is then formed  
 4 from SCI, where  $Y_{OH} = Y_{OH}^{CI^*} + Y_{OH}^{SCI}$  and hence  $Y_{OH}^{SCI} \approx 0.2$ .

5 We adopt a value for  $Y_{SCI}$  of 0.4, as argued in section 3.2. The SCI formed do not all  
 6 decompose to OH, e.g. *anti*-CI tend to form esters instead. We label all SCI able to yield OH  
 7 as  $SCI_{syn}$ , without mandating a speciation but following the observation that *syn*-CI usually  
 8 yield OH through the vinylhydroperoxide channel. The total SCI yield is then divided into a  
 9 fraction,  $Y_{syn}$ , forming  $SCI_{syn}$ , and the remainder,  $Y_{anti}$ , forming non-OH-generating SCI. Little  
 10 information is available on the  $Y_{syn}:Y_{anti}$  ratio, with only a few theoretical calculations on  
 11 smaller alkenes and a few monoterpenes (Rathman et al., 1999; Fenske et al., 2000b; Kroll et  
 12 al., 2002; Nguyen et al., 2009b; Nguyen et al., 2009a). For most of these compounds the ratio  
 13 of *syn*- to *anti*-SCI is between 0.2 and 1.0 (Rickard et al., 1999) where a larger fraction of  
 14 *syn*- to *anti*-SCI, or vice versa, will depend on the single alkene. As there is no information  
 15 available for the VOC included in this study, we estimate the ratio of  $Y_{syn}$  to  $Y_{anti}$  as 1:1. This  
 16 number avoids overestimating the impact of SCI in the OH production and, using the *syn* to  
 17 *anti* range indicated above, would cause a variation in the final [SCI] estimate of maximum  
 18 20 %, (see eq. 7 and Figure 3) well below the total uncertainty of the result.

19 The production of OH from  $SCI_{syn}$  formed from VOC not included in the OH budget is then  
 20  $k_{OH} \times [SCI_{syn}]$ , where we estimate  $k_{OH} \approx 20 \text{ s}^{-1}$  as measured by Novelli et al. (2014b) for *syn*-  
 21  $CH_3CHOO$ , and where the steady state concentration of the  $SCI_{syn}$ ,  $[SCI_{syn}]$ , is determined by  
 22 the ratio of the formation processes and the sum  $L_{SCI_{syn}}$  of the loss processes already defined  
 23 above:

$$[SCI_{syn}] = \frac{k_{voc+O_3} \times [VOC_{unidentified}] \times [O_3] \times Y_{SCI} \times Y_{syn}}{L_{SCI_{syn}}} \quad (6)$$

Merging the above equations, expressing the measured OH production from unknown sources as the sum of direct OH production from  $CI^*$  and indirect from  $SCI_{syn}$ , we obtain:

$$P_{unexplained}^{OH} = k_{voc+O_3} \times [VOC_{unidentified}] \times [O_3] \times \left( Y_{OH}^{CI^*} + Y_{SCI} \times Y_{syn} \times \frac{k_{OH}}{L_{SCI_{syn}}} \right) \quad (7)$$

The measured  $P_{OH}^{unexplained}$  and  $[O_3]$ , and the estimates of the other parameters allow us to calculate the factor  $k_{voc+O_3} \times [VOC_{unidentified}]$ . Substituting this factor into Eq. 6 yields an estimate of the steady state concentration of  $SCI_{syn}$ . With a value for  $P_{OH}^{unexplained}$  of  $1.0 \times 10^6$  molecules  $cm^{-3} s^{-1}$  as observed for low reactivity episodes and at night during HUMPPA, a steady state concentration of  $SCI_{syn}$  of  $(2.0 \pm 2.0) \times 10^4$  molecules  $cm^{-3}$  is calculated. For high reactivity episodes during HUMPPA-COPEC 2010, the missing  $P_{OH}^{unexplained}$  of  $2.0 \times 10^7$  molecules  $cm^{-3} s^{-1}$  results in a SCI concentration of  $(4.0 \pm 4.0) \times 10^5$  molecules  $cm^{-3}$ . To obtain the total SCI concentration, we then need to add the non-OH-producing SCI. Here we assume that these are mostly *anti*-SCI or  $H_2COO$ , both of which react rather quickly with  $H_2O$  or  $(H_2O)_2$  (Taatjes et al., 2013;Chao et al., 2015;Lewis et al., 2015), and that their contribution can be neglected. We thus obtain that  $[SCI] \approx [SCI_{syn}]$ . To this we add the SCI concentration calculated from the measured unsaturated VOC (section 3.2),  $(5.0 \pm 4.0) \times 10^3$  molecules  $cm^{-3}$ , to obtain the SCI formed from all VOC.

For HOPE 2012 it is difficult to accurately derive an OH budget due to the lack of information on the HONO concentration, which can represent an important primary source of OH. A detailed analysis of the OH production and loss during the campaign thus requires a

1 detailed model study to derive HONO concentrations, which is outside the scope of this  
2 paper. Hence, an estimate on the SCI from a possible missing OH production rate during the  
3 HOPE 2012 campaign is not included here.

4 Equation 7, for a given set of yields, unimolecular decomposition rates and SCI losses, allows  
5 the estimate of the relative contribution of SCI and  $\text{Cl}^*$  to the total production rate of OH  
6 from the ozonolysis of VOC. With the yields considered in this study and for a unimolecular  
7 decomposition rate of SCI into OH of  $20 \text{ s}^{-1}$ , the SCI would contribute up to 12 % to the total  
8 formation of OH from ozonolysis of VOC in both environments. This indicates that the SCI  
9 do not have a large impact in the production of OH radicals and at the same time emphasizes  
10 how important a realistic estimate of VOC concentration is for modeling the OH radical as  
11 already underlined by (Hens et al., 2014).

### 12 **3.5 Robustness of the [SCI] estimates**

13 Figure 3 summarises the steady state concentration of SCI calculated on the basis of the  
14  $\text{H}_2\text{SO}_4$  budget, the measured unsaturated VOC concentration and OH reactivity (R), and the  
15 OH budget for the HUMPPA-COPEC 2010 and HOPE 2012 campaigns. By considering the  
16 lower and the highest values estimated from the measured VOC and from the missing  $\text{H}_2\text{SO}_4$   
17 oxidant for both campaigns, respectively, the steady state concentration of SCI is calculated  
18 to be between  $5.0 \times 10^3$  and  $2.0 \times 10^6 \text{ molecules cm}^{-3}$  for the boreal forest environment during  
19 the HUMPPA-COPEC 2010 campaign and between  $7.0 \times 10^3$  and  $1.0 \times 10^6 \text{ molecules cm}^{-3}$   
20 for rural Germany during the HOPE 2012 campaign (Table 2). The SCI concentrations  
21 calculated using these approaches represent a best-effort estimate made for the environments  
22 studied here based on the available data; due to the many uncertainties related to the  
23 chemistry of SCI both in production and loss processes these estimates span about two orders  
24 of magnitude.

1 The estimate of the SCI concentration from the sulfuric acid budgets relies on the rate of  
 2 oxidation of SO<sub>2</sub> to H<sub>2</sub>SO<sub>4</sub>. As indicated in section 3.1, two significantly different rate  
 3 coefficients for the reaction of SCI with SO<sub>2</sub> are currently available. One coefficient is high, ~  
 4  $3.3 \pm 2.0 \times 10^{-11} \text{ cm}^3 \text{ molecule}^{-1} \text{ s}^{-1}$ , while the other is several orders of magnitude lower,  $5.0$   
 5  $\times 10^{-13} \text{ cm}^3 \text{ molecule}^{-1} \text{ s}^{-1}$ . Justifications of the differences in the values due to the diverse  
 6 procedures, i.e. direct detection of SCI + SO<sub>2</sub> for the high rate coefficient and detection of  
 7 H<sub>2</sub>SO<sub>4</sub> for the lower one, are difficult, while recent measurements tend to agree with the  
 8 highest value. This casts doubts on the highest obtained SCI concentrations of  $\sim 10^6$   
 9 molecules cm<sup>-3</sup>. In addition, the remaining three estimates strongly depend on the yield of  
 10 SCI,  $k_{\text{VOC}+\text{O}_2}$  and  $L_{\text{SCI}_{\text{syn}}}$ . Among these, the parameter with the highest uncertainty is the loss  
 11 rate of *syn*-SCI,  $L_{\text{SCI}_{\text{syn}}}$ , as it is based on relatively few studies, which report large differences  
 12 between the observations. In this study, a value of 40 s<sup>-1</sup> and of 32 s<sup>-1</sup>, based on previous  
 13 model analysis (Novelli et al., 2014b), for the HUMPPA-COPEC 2010 and HOPE 2012  
 14 campaigns respectively, were used. Recent work (Smith et al., 2016; Fang et al., 2016a; Long  
 15 et al., 2016) suggests a faster unimolecular decomposition rate for the acetone oxide Criegee  
 16 intermediate, exceeding 10<sup>2</sup> s<sup>-1</sup> in ambient conditions. It is currently not clear whether this  
 17 rate applies to more substituted SCI as formed from monoterpenes but the use of these higher  
 18 decomposition rate in the model by (Novelli et al., 2014b) would result in a total  $L_{\text{SCI}_{\text{syn}}}$  of ~  
 19 110 s<sup>-1</sup>. This loss rate would decrease the estimated SCI concentration by almost a factor of 3,  
 20 closer to the lower estimates not exceeding 10<sup>5</sup> molecule cm<sup>-3</sup>; this also casts doubt on the  
 21 highest estimates given in Figure 3. Therefore, an average estimated SCI concentration of  
 22 about  $5 \times 10^4 \text{ molecules cm}^{-3}$ , with an order of magnitude uncertainty, is considered more  
 23 appropriate for both campaigns.

24

## 4 The source of the OH background signal

In this section we examine the background OH signal,  $\text{OH}_{\text{bg}}$  (Novelli et al., 2014b) measured during the two field campaigns discussed in the previous sections. In particular, we examine if this signal is consistent with the SCI chemistry and concentrations indicated above.

### 4.1 Correlation of $\text{OH}_{\text{bg}}$ with temperature

The time series of the background OH signal measured during the HUMPPA-COPEC 2010 and HOPE 2012 campaigns are shown together with temperature and  $J(\text{O}^1\text{D})$  values in Fig. 4. Increases and decreases in the  $\text{OH}_{\text{bg}}$  signal follow the temperature changes. During the HUMPPA-COPEC 2010 campaign the  $\text{OH}_{\text{bg}}$  shows a strong correlation with temperature (Fig. 5) with a correlation coefficient  $R = 0.8$  for the exponential fit. The exponential dependency with temperature is in agreement with data shown by Di Carlo et al. (2004) for the unexplained OH reactivity and indicates that the species responsible for the  $\text{OH}_{\text{bg}}$  strongly correlate with emission of biogenic VOC (BVOC) such as monoterpenes and sesquiterpenes, which have been shown to also exponentially depend on temperature (Guenther et al., 1993; Duhl et al., 2008; Hakola et al., 2003). This suggests that  $\text{OH}_{\text{bg}}$  is directly related to BVOC chemistry. The relationship between  $\text{OH}_{\text{bg}}$  and temperature during the HOPE 2012 campaign is less obvious. It is possible to observe a weakly exponential correlation between the two ( $R = 0.51$ , Fig. SI-10) but there is very large scatter in the data. It is worthwhile to underline the differences between the two environments. The forest in Finland is essentially pristine and BVOC dominated while in southern Germany a large fraction of non-biogenic VOC was observed. The lack of a clear exponential correlation between  $\text{OH}_{\text{bg}}$  and temperature during the HOPE 2012 campaign could suggest different precursors or a different origin for the  $\text{OH}_{\text{bg}}$  within the two environments.



During both campaigns a negligible correlation,  $R = 0.2$ , was observed between background OH and  $J(O^1D)$ . This suggests that the  $OH_{bg}$  does not primarily originate from photolabile species.

## 4.2 Correlation of $OH_{bg}$ with unexplained OH reactivity

As described in section 3.3, during the HUMPPA-COPEC 2010 campaign high average OH reactivity was observed ( $\sim 9 \text{ s}^{-1}$ ), of which between 60 % and 90 % cannot be explained by the loss processes calculated from the measured species (Nölscher et al., 2012). A large unexplained fraction of the reactivity has often been observed, especially in forested environments (Di Carlo et al., 2004; Sinha et al., 2008; Edwards et al., 2013) indicating a large fraction of undetected BVOC and/or secondary oxidation products. The  $OH_{bg}$  shows some correlation with the measured unexplained OH reactivity at 18 m, for the period on the ground ( $R = 0.4$ ), and the measured unexplained OH reactivity at 24 m, for the period on the tower ( $R = 0.4$ ) (Fig. 6). If we consider only night time data, i.e.  $J(O^1D) \leq 3.0 \times 10^{-6} \text{ s}^{-1}$  (Hens et al., 2014), we obtain better agreement between the two datasets for both ground and tower periods. During the night a large fraction of observed OH production (section 3.4) could not be explained, which can tentatively be attributed to formation of OH from ozonolysis of BVOC, suggesting that the background OH could be related to such a process. Correlation between the  $OH_{bg}$  and the OH reactivity was also observed in a study by Mao et al. (2012) in a Ponderosa pine plantation (California, Sierra Nevada Mountains) dominated by isoprene where even higher OH reactivity was observed ( $\sim 20 \text{ s}^{-1}$ ).

During the HOPE 2012 campaign such a correlation with the unexplained OH reactivity was not observed ( $R = 0.1$ ). The OH reactivity was, on average, 3 times less than during the campaign in Finland and, as shown in section 3.3, 50 % can be explained by reaction of OH with methane, formaldehyde, acetaldehyde, inorganic compounds ( $NO_x$ ,  $SO_2$ , CO) and

anthropogenic VOC. On average only 17 % of the OH reactivity is caused by reaction of OH with BVOC in this environment (Fig SI-8), dropping to 10 % during the night. The unexplained OH reactivity is not influenced by distinguishing between day and night time data suggesting a small contribution of non-measured BVOC. As this site is more strongly affected by anthropogenic emissions (Table SI-2) compared to the site in Finland, assuming that the  $\text{OH}_{\text{bg}}$  originates from BVOC driven chemistry, a lack of correlation between  $\text{OH}_{\text{bg}}$  and OH reactivity can be expected.

### 4.3 Correlation of $\text{OH}_{\text{bg}}$ with ozonolysis chemistry

During the HUMMPA-COPEC 2010 campaign a high correlation with  $\text{O}_3$ ,  $R = 0.7$  (Fig. SI-11), indicates that background OH likely originates from ozonolysis processes. A comparison of background OH with the product of ozone concentration, measured unsaturated VOC concentration and their ozonolysis rate coefficient does not show the same relationship. No correlation ( $R = 0.05$ ) is found by using the measured BVOC concentrations (Table SI-1). As most of the OH reactivity remains unexplained, with measured BVOC comprising less than 10 % of the measured OH reactivity (Fig SI-6, Table SI-2), the lack of correlation could suggest that the VOC responsible for the formation of SCI detected by the HORUS instrument are likely part of the large fraction of unmeasured species to which a correlation was reported in the previous section.

During HOPE 2012 a weak correlation was observed between background OH and ozone ( $R = 0.5$ , fig. SI-12).

This campaign, from July 10<sup>th</sup> to August 19<sup>th</sup> 2012, encompasses a time period, from 1<sup>st</sup> to 3<sup>rd</sup> of August 2012, which was characterized by tree cutting in the vicinity of the measurement

1 site. During this period a significantly larger fraction of unexplained OH reactivity, up to 40  
2 % (Fig. SI-13), was observed. The relative contribution of measured BVOC and inorganic  
3 compounds did not change, while the presence of unidentified BVOC emitted from the trees  
4 as a result of the stress induced on the plants from the cutting activity, caused the larger  
5 fraction of unexplained reactivity. Figure 7 shows the correlation between  $\text{OH}_{\text{bg}}$  and the  
6 product  $k_{\text{O}_3}[\text{VOC}][\text{O}_3]$  of measured unsaturated VOC concentration (Table SI-1),  $[\text{O}_3]$  and  
7 the relevant ozonolysis rate coefficients. In red are depicted the data points belonging to the  
8 tree cutting period, which naturally correspond to a larger  $\text{OH}_{\text{bg}}$  concentration for similar  
9 concentrations of measured VOC during the rest of the campaign, as the additional  
10 contribution from the non-identified BVOC is neglected. The overall correlation appears to  
11 be pretty poor in particular due to the few points scattering in the lower right corner. These  
12 points all belong to three consecutive days, from 26<sup>th</sup> to 28<sup>th</sup> of July, which were  
13 characterised by high temperature and large concentrations of BVOC (Table SI-3). As  
14 noticeable in Figure 4, during those three days the  $\text{OH}_{\text{bg}}$  strongly deviates from the  
15 temperature trends and reaches lower values. At present, the reason for such a low  
16 concentration of  $\text{OH}_{\text{bg}}$ , during a period which should favour its formation if it originates from  
17 SCI, is unclear. The instrument was left unattended at the site and the drop in the quality of  
18 the signals required its shutdown on the evening of the 28<sup>th</sup> of July. However, as no evidence  
19 was found to suggest an error in the data the points have not been omitted. Excluding that  
20 period yields a correlation factor of  $R = 0.65$ . The correlation line intercept could arise for a  
21 number of reasons. Unmeasured components of the OH reactivity (i.e. unspiciated VOCs)  
22 are not accounted for in the calculation, and doing so would shift the data to higher  $[\text{VOC}]$ ,  
23 decreasing the positive intercept. This is also consistent with a higher intercept for the cutting  
24 tree period where a larger unexplained OH reactivity was observed. It is also conceivable that

the intercept is in part due to an additional, non-ozonolysis source of background OH. One candidate for the night time periods could be NO<sub>3</sub> as found in the work by Fuchs et al. (2016). Unfortunately, there was no measurement of the NO<sub>3</sub> radical during the HOPE 2012 campaign, but based on previous studies at the site (Handisides et al., 2003), a concentration up to 14 pptv of NO<sub>3</sub> could be present and could have a detectable impact.

Apart from the possible partial origin of OH<sub>bg</sub> from NO<sub>3</sub> or other interferences, there are also indications that the background OH could originate from ozonolysis of unsaturated biogenic compounds. The correlation analysis requires that all VOCs are accounted for, and omitting large contributions from unspciated VOCs, as evidenced e.g. by OH reactivity measurements, can be expected to reduce the correlation as observed in the case of HUMPPA-COPEC 2010. The reason for the lack of correlation during the period from 26<sup>th</sup> to 28<sup>th</sup> July 2012 during HOPE-2012 characterised by large BVOC emissions remains unclear.

#### **4.4 Correlation of OH<sub>bg</sub> with P(H<sub>2</sub>SO<sub>4</sub>)<sub>unex</sub>**

During both campaigns, measurements of H<sub>2</sub>SO<sub>4</sub>, SO<sub>2</sub>, OH and CS (condensation sink) were performed allowing the calculation of the sulfuric acid budget in the gas phase. As shown by Mauldin III et al. (2012), during the HUMPPA-COPEC 2010 campaign the well-known SO<sub>2</sub> oxidation process by OH (Wayne, 2000) (Eq. 1) was not sufficient to explain the measured concentration of H<sub>2</sub>SO<sub>4</sub>. As shown in section 3.1, half of the production rate of H<sub>2</sub>SO<sub>4</sub>, ~ 1 x 10<sup>4</sup> molecules cm<sup>-3</sup> s<sup>-1</sup>, cannot be explained by reaction with OH radicals (Fig. 8). The missing oxidant is assumed to be SCI, as discussed in section 3.1, because of their fast reaction rate with SO<sub>2</sub>. As our hypothesis about the origin of the OH<sub>bg</sub> supports this assumption, we compared the [H<sub>2</sub>SO<sub>4</sub>]<sub>unex</sub> observed during the HUMPPA-COPEC 2010

1 campaign with the  $\text{OH}_{\text{bg}}$  multiplied by  $\text{SO}_2$  for the ground-based period when the instruments  
2 (HORUS and CIMS) measured side-by-side (Fig. 9). The two datasets indicate a correlation  
3 coefficient of  $R = 0.6$  suggesting that whichever species is responsible for the oxidation of  
4  $\text{SO}_2$  is related to the formation of OH within the HORUS instrument.  
5 Note that for the HOPE 2012 campaign the same budget calculation shows only a small  
6 fraction (10 %) of unexplained  $\text{H}_2\text{SO}_4$  production rate (Fig. 1).  
7 Assuming SCI to be the unknown  $\text{SO}_2$  oxidant, the results observed in both campaigns are in  
8 agreement with the modeling study by Boy et al. (2013), who analyzed measurements at the  
9 same sites described in this study. Similar to our result, they found a larger contribution of  
10 SCI in the formation of  $\text{H}_2\text{SO}_4$  for the boreal forest compared to rural Germany. As the OH  
11 concentration differs by, on average, less than 50 % between the two environments, a similar  
12 concentration of SCI in HOPE to that calculated for HUMPPA-COPEC 2010 would  
13 contribute up to 30 % in the formation of  $\text{H}_2\text{SO}_4$ . However, the  $\text{H}_2\text{SO}_4$  budget during this  
14 campaign can approximately be closed by only considering the measured OH concentrations,  
15 suggesting that the concentration of SCI in this environment is smaller than that during the  
16 HUMPPA-COPEC 2010 campaign. This is consistent with the calculation in section 3 based  
17 on the smaller reactivity and hence smaller VOC concentration in this environment

#### 18 **4.5 Scavenging experiments**

19 A series of scavenging tests of the  $\text{OH}_{\text{bg}}$  was performed during the HOPE 2012 campaign to  
20 help identify the interfering species.  $\text{SO}_2$  was chosen as scavenger for the species causing the  
21  $\text{OH}_{\text{bg}}$ , as it has been shown in several laboratory studies to react quickly with SCI ( $k \sim 3.3 \times$   
22  $10^{-11} \text{ cm}^3 \text{ molecule}^{-1} \text{ s}^{-1}$ ) mostly independently of their structure (Taatjes et al., 2014). The  
23 injection of  $\text{SO}_2$  was performed through the IPI system (Novelli et al., 2014a) together with  
24 an OH scavenger. First the OH scavenger propane was injected within IPI to remove the

1 atmospheric OH; subsequently, SO<sub>2</sub> was injected in addition to the OH scavenger (Fig. 10).  
2 A set of experiments were performed at the end of the campaign resulting in the depletion of  
3 the OH<sub>bg</sub> signal as shown in Figure 10. The concentration of SO<sub>2</sub> is small enough not to  
4 scavenge SCI inside the low pressure section of the instrument, nor is it additionally  
5 removing atmospheric OH within the IPI system as the lifetime of OH by reaction with SO<sub>2</sub>  
6 is 200 times that of propane. With the addition of SO<sub>2</sub> ( $1 \times 10^{13}$  molecules cm<sup>-3</sup> in the sampled  
7 air) it is possible to suppress the OH<sub>bg</sub> signal from the instrument to within the zero noise,  
8 indicating that the OH<sub>bg</sub> signal originates from an SCI-like species that reacts with SO<sub>2</sub> and  
9 decomposes unimolecularly to OH. Similar results were obtained in later field campaigns;  
10 this will be discussed in the pertaining upcoming publications. Note that it is not possible to  
11 link the signal strength directly to an OH or precursor concentration, as analysed in the  
12 following section.

13

#### 14 **4.6 SCI as a source of background OH**

15 During the HUMPPA-COPEC 2010 campaign the background OH showed a strong  
16 exponential relationship with temperature ( $R = 0.8$ ) and it correlates with unexplained OH  
17 reactivity ( $R = 0.5$ ), which suggests correlation with BVOC, with ozone ( $R = 0.7$ ), and also  
18 with the  $P(H_2SO_4)_{unex}$  ( $R = 0.6$ ). During the HOPE 2012 campaign a weak exponential  
19 correlation with temperature was recognized ( $R = 0.5$ ) but no correlation was observed with  
20 OH reactivity. The OH<sub>bg</sub> correlated with the product of ozone and unsaturated VOC for most  
21 of the campaign ( $R = 0.6$ ) although not for a period of three days at the end of July with  
22 partly higher BVOC-O<sub>3</sub> turnover. In addition, during HOPE 2012 the OH<sub>bg</sub> signal was  
23 scavenged by the addition of SO<sub>2</sub>.

1 All evidence presented indicates that substantial parts of the OH<sub>bg</sub> originate from a species  
2 formed during the ozonolysis of unsaturated VOC that decomposes into OH, is removable by  
3 SO<sub>2</sub> and, if present in a significant concentration, increases the H<sub>2</sub>SO<sub>4</sub> production. We are  
4 currently not aware of any chemical species, other than SCI, known to oxidise SO<sub>2</sub> at a fast  
5 enough rate and also decompose into OH. In addition, HORUS was shown to be sensitive to  
6 the OH formed after unimolecular decomposition of SCI in the low-pressure region of the  
7 instrument (residence time 2 ms) in controlled laboratory studies (Novelli et al., 2014b).  
8 During the HUMPPA-COPEC 2010 campaign, the correlation with OH reactivity improved  
9 when considering only data during night time, the period during which a higher fraction of  
10 the production rate of OH could not be accounted for (Hens et al., 2014). Indeed, during the  
11 night recycling via HO<sub>2</sub>+NO is low due to the negligible NO concentration, therefore a  
12 different path of formation of OH is expected. One likely path could be the formation of OH  
13 from excited and stabilised CI formed from ozonolysis of unsaturated compounds.

14 The considerations above are all consistent with the hypothesis that OH<sub>bg</sub> largely originates  
15 from unimolecular decomposition of SCI in the field as well as in the laboratory.

16 Attempts to analyse the absolute concentration of SCI based on our OH<sub>bg</sub>, however, indicates  
17 that this hypothesis is not without difficulties. A particular problem is that to date no method  
18 is available to produce and quantify a known concentration of a specific SCI conformer,  
19 which precludes the absolute calibration of SCI-generated OH. *A priori*, it seems unlikely  
20 that the IPI-LIF-FAGE instrument calibration factor for ambient OH, i.e. sampled from  
21 outside the instrument through the nozzle, is identical to the sensitivity for OH generated  
22 inside. The transmission factor through our nozzle pinhole is currently not known for OH  
23 radicals; the calibration factor used for ambient OH accounts for this transmission as well as  
24 for e.g. OH losses on the walls, alignment of the white cell, transmission optics, and response

1 of the MCP. These last three factors should affect the OH generated from any interfering  
2 species similarly, while wall losses and transmission through the pinhole are different and  
3 possibly also differ between SCI conformers. Additionally, different SCI vary in their  
4 unimolecular decomposition rates and hence affect calibration by a different time-specific  
5 OH yield. For example, theoretical studies (Vereecken and Francisco, 2012) and laboratory  
6 experiments (Smith et al., 2016) indicate that acetone oxide will decompose faster than *syn*-  
7 acetaldehyde oxide causing the formation of a different amount of OH, which in turn will  
8 also be affected by different loss rates in the low pressure segment of the instrument. Thus, it  
9 is not possible to convert the internal OH to an absolute SCI concentration since the mixture  
10 of SCI is not known. At best one could obtain an "average" sensitivity factor, if one knew the  
11 OH<sub>bg</sub> formed from a series of reference SCI conformers, and if the ambient SCI speciation is  
12 known and not too strongly dependent on reaction conditions. To further illustrate the need of  
13 a SCI-specific calibration, we try to simply calculate the external [SCI] from the internal  
14 OH<sub>bg</sub> signal strength, calibrated based on the combined experimental and modelling study by  
15 Novelli et al. (2014b). For a SCI mixture that behaves identical to *syn*-CH<sub>3</sub>CHOO, the OH<sub>bg</sub>  
16 from the HUMPPA-COPEC 2010 campaign would then indicate an external [SCI]  $\geq 2 \times 10^7$   
17 molecules cm<sup>-3</sup>, well above the estimates presented in section 3. Moreover, the observed  
18 OH<sub>bg</sub> signal interpreted in this way would imply an ambient OH production exceeding  $4 \times$   
19  $10^8$  molecules cm<sup>-3</sup> s<sup>-1</sup>, clearly in disagreement with known chemistry, and also inconsistent  
20 with our estimates (Table 2). If we assume a faster decomposition rate for the SCI of 200 s<sup>-1</sup>,  
21 a higher fraction of the SCI decomposes in the low-pressure region, i.e. 80 % compared to 25  
22 % for  $k_{\text{uni}} = 20$  s<sup>-1</sup>. This leads to a higher OH signal per SCI, and from this a [SCI] of  $4.0 \times$   
23  $10^6$  molecules cm<sup>-3</sup>, though the implied ambient OH production would remain significantly  
24 too high. Thus, the conversion of the OH signal to an absolute concentration of ambient SCI



1 is not unambiguous without full SCI speciation and knowledge of their chemical kinetics.  
2 Note furthermore that these [SCI] estimates would represent a lower limit as we only observe  
3 SCI that decompose to OH, whereas e.g. *anti*-SCI convert to acids/esters.

4 In an effort to work towards SCI-specific calibration, we probed the transmission of OH and  
5 *syn*-CH<sub>3</sub>CHOO through the nozzles and the low-pressure region in the instrument, with  
6 explorative laboratory tests using a traditional nozzle and a molecular beam skimmer nozzle,  
7 where the latter has much thinner sidewalls and a significantly narrower gas expansion,  
8 strongly reducing wall contact. The laboratory test showed that the OH radical has a 23 %  
9 higher transmission through the molecular beam nozzle compared to the traditional nozzle.

10 The *syn*-acetaldehyde oxide did not show any statistical difference in the transmission  
11 between the two nozzles. This indicates that (a) SCI and OH have a different transmission  
12 efficiency and most likely different wall losses, underlining that the OH calibration factor is  
13 not applicable to SCI for ambient measurements, and (b) that the calibration factor for OH  
14 obtained for ambient OH alone does not allow the quantification of the absolute OH  
15 concentration in the low-pressure section of the FAGE instrument. This is the fundamental  
16 reason why the earlier simple estimate of [SCI] and OH production leads to strong over-  
17 estimations.

18 In addition to the above effects, one should also consider that OH-production from SCI in the  
19 low-pressure section might be catalysed to proceed at rates beyond their ambient counterpart,  
20 biasing our interpretation of their ambient fate. The catalysis might involve wall-induced  
21 isomerisation of the higher-energy *anti*-SCI to the more stable, OH-producing *syn*-SCI,  
22 which would artificially increase the *syn:anti* ratio. Another possibility is the evaporation of  
23 clusters stabilizing the SCI, as it is known that SCI efficiently form complexes with many  
24 compounds, including water, acids, alcohols, hydroperoxides, HO<sub>x</sub> radicals, etc. (Vereecken

1 and Francisco, 2012). Redissociation of secondary ozonides (SOZ) seems less important,  
2 except perhaps the SOZ formed with CO<sub>2</sub> (Aplincourt and Ruiz-López, 2000), which has no  
3 alternative accessible unimolecular channels. At present, insufficient (if any) information is  
4 available to assess the impact of such catalysis.

5 Taking into account the factors considered above, and assuming that the estimates for the SCI  
6 concentration in both environments are correct, it appears unlikely that SCI are responsible  
7 for such a large OH<sub>bg</sub> signal as observed by the HORUS instrument. If SCI were to be solely  
8 responsible for the OH<sub>bg</sub> signal, the HORUS instrument would need to be far more sensitive  
9 to the detection of SCI than to the detection of OH radicals by, for example, pinhole losses  
10 that are 100 times smaller for SCI than for OH radicals. The evident discrepancy between the  
11 qualitative evidence in support of the SCI hypothesis and the current quantitative difficulty in  
12 reconciling the OH<sub>bg</sub> signal with the estimated ambient concentration of SCI does not allow  
13 an unequivocal identification of the origin of the OH<sub>bg</sub> within our system. It cannot be  
14 excluded that multiple species are contributing to the OH<sub>bg</sub> signal. NO<sub>3</sub> chemistry during  
15 night time has been identified as a possible source of OH<sub>bg</sub> in the LIF-FAGE instrument of  
16 the FZ-Jülich (Fuchs et al., 2016). However, in the case of the large observed night time OH<sub>bg</sub>  
17 concentrations during HUMPPA-COPEC 2010, the measured night time NO<sub>3</sub> concentrations  
18 were below 1 ppt and therefore too small to explain the observed OH<sub>bg</sub>.

## 20 **5 Conclusions**

21 We estimated a steady state concentration of SCI for the HUMPPA-COPEC 2010 and the  
22 HOPE 2012 campaigns based on a large dataset. Starting from four different approaches, i.e.  
23 based on unaccounted (i.e. non-OH) H<sub>2</sub>SO<sub>4</sub> oxidant, measured VOC concentrations,

1 unexplained OH reactivity or unexplained production rates of OH, we estimated the  
2 concentration of SCI to be between  $\sim 10^3$  and  $\sim 10^6$  molecules  $\text{cm}^{-3}$ . The highest values in  
3 this range are linked to an assumed low rate coefficient for SCI + SO<sub>2</sub> of  $5.0 \times 10^{-13}$  cm<sup>3</sup>  
4 molecule<sup>-1</sup> s<sup>-1</sup> (see section 3.1), which is at odds with a larger body of more direct  
5 measurements on this rate coefficient. Hence, higher SCI values appear to be relatively less  
6 likely. We thus obtain an average SCI concentration of about  $5.0 \times 10^4$  molecules  $\text{cm}^{-3}$ , with  
7 an order of magnitude uncertainty, for both campaigns. At such concentrations, SCI are  
8 expected to have a significant impact on H<sub>2</sub>SO<sub>4</sub> chemistry during the HUMPPA-COPEC  
9 2010 campaign while during the HOPE 2012 campaign their impact is much smaller and  
10 possibly negligible. Additionally, it was shown that, based on the yields and unimolecular  
11 decomposition rate applied in this study, SCI do not have a large impact on the OH  
12 production compared to the direct OH generation from ozonolysis of unsaturated VOC.  
13 During both campaigns, the IPI-LIF-FAGE instrument detected an OH background signal  
14 that originates from decomposition of one or more species inside the low pressure region of  
15 the instrument. The source compound of the OH<sub>bg</sub> was shown to be unreactive towards  
16 propane but to be removed by SO<sub>2</sub>, and a relationship was found with the unaccounted H<sub>2</sub>SO<sub>4</sub>  
17 production rate. It correlates with temperature in the same way as the emission of terpenes  
18 and, in most but not all measurements periods, with the product of unsaturated VOC and  
19 ozone as well as with the OH reactivity. While it is not possible at the moment to  
20 unequivocally state that OH<sub>bg</sub> originates from stabilised Criegee intermediates, the  
21 observations are consistent with known SCI chemistry. The contribution of SCI to the  
22 observed OH<sub>bg</sub> cannot be quantified until a calibration scheme for SCI in the IPI-FAGE  
23 system has been developed.

The predicted SCI concentrations derived in this study are low, likely not exceeding  $10^5$  molecule  $\text{cm}^{-3}$ , therefore, the presence of SCI is unlikely to have a large impact on atmospheric chemistry; the main exception appears to be  $\text{H}_2\text{SO}_4$  production in selected environments.

## Acknowledgements

LV was supported by the Max Planck Graduate Centre (MPGC) with the Johannes Gutenberg-Universität Mainz.

Work during HUMPPA-COPEC was supported by the Hyytiälä site engineers and staff. Support of the European Community Research Infrastructure Action under the FP6 "Structuring the European Research Area" Programme, EUSAAR Contract No RII3-CT-2006-026140 is gratefully acknowledged. The HUMPPA-COPEC 2010 campaign measurements and analyses were supported by the ERC Grant ATMNUCLE (project No 227463), Academy of Finland Centre of Excellence program (project No 1118615), , Academy of Finland Centre of Excellence in Atmospheric Science – From Molecular and Biological processes to The Global Climate' (ATM), 272041, the European integrated project on Aerosol Cloud Climate and Air Quality Interactions EUCAARI (project No 036833-2), the EUSAAR TNA (project No 400586), and the IMECC TA (project No 4006261).

The work during HOPE 2012 was supported by the scientists and staff of DWD Hohenpeißenberg whom we would like to thank for providing the "platform" and opportunity to perform such campaign. In particular, we thank, Anja Werner, Jennifer Englert and Katja Michl for the VOC measurements, Stephan Gilge for the trace gases measurements and Georg Stange for running the CIMS.

We also would like to thank Markus Rudolf for much technical support and guidance, Eric Regelin and Umar Javed for the numerous scientific discussions, Petri Keronen for providing meteorological and trace gas concentration data from Hyytiälä during the HUMPPA-COPEC 2010 and Thorsten Berndt for providing the data to re-evaluate the rate coefficient between SCI and  $\text{SO}_2$ .

1

2 **References**

- 3 Aalto, P., Hämeri, K., Becker, E. D. O., Weber, R., Salm, J., Mäkelä, J. M., Hoell, C.,  
4 O'Dowd, C. D., Karlsson, H., Hansson, H.-C., Väkevä, M., Koponen, I. K., Buzorius, G., and  
5 Kulmala, M.: Physical characterization of aerosol particles during nucleation events, *Tellus*  
6 *B*, 53, 344-358, 10.1034/j.1600-0889.2001.530403.x, 2001.
- 7 Ahrens, J., Carlsson, P. T., Hertl, N., Olzmann, M., Pfeifle, M., Wolf, J. L., and Zeuch, T.:  
8 Infrared detection of Criegee intermediates formed during the ozonolysis of beta-pinene and  
9 their reactivity towards sulfur dioxide, *Angew Chem Int Ed Engl*, 53, 715-719,  
10 10.1002/anie.201307327, 2014.
- 11 Amédro, D.: Atmospheric measurements of OH and HO<sub>2</sub> radicals using FAGE :  
12 Development and deployment on the field, Université Lille1 - Sciences et Technologies,  
13 Tokyo Metropolitan University, 2012.
- 14 Anglada, J. M., Bofill, J. M., Olivella, S., and Solé, A.: Unimolecular Isomerizations and  
15 Oxygen Atom Loss in Formaldehyde and Acetaldehyde Carbonyl Oxides. A Theoretical  
16 Investigation, *J Am Chem Soc*, 118, 4636-4647, 10.1021/ja953858a, 1996.
- 17 Anglada, J. M., Gonzalez, J., and Torrent-Sucarrat, M.: Effects of the substituents on the  
18 reactivity of carbonyl oxides. A theoretical study on the reaction of substituted carbonyl  
19 oxides with water, *Phys Chem Chem Phys*, 13, 13034-13045, 2011.
- 20 Anglada, J. M., and Sole, A.: Impact of water dimer on the atmospheric reactivity of carbonyl  
21 oxides, *Phys Chem Chem Phys*, 10.1039/C6CP02531E, 2016.
- 22 Aplin-court, P., and Ruiz-López, M. F.: Theoretical Investigation of Reaction Mechanisms for  
23 Carboxylic Acid Formation in the Atmosphere, *J Am Chem Soc*, 122, 8990-8997,  
24 10.1021/ja000731z, 2000.
- 25 Atkinson, R., Baulch, D. L., Cox, R. A., Crowley, J. N., Hampson, R. F., Hynes, R. G.,  
26 Jenkin, M. E., Rossi, M. J., and Troe, J.: Evaluated kinetic and photochemical data for  
27 atmospheric chemistry: Volume I - gas phase reactions of Ox, HOx, NOx and SOx species,  
28 *Atmos. Chem. Phys.*, 4, 1461-1738, 10.5194/acp-4-1461-2004, 2004.
- 29 Atkinson, R., Baulch, D. L., Cox, R. A., Crowley, J. N., Hampson, R. F., Hynes, R. G.,  
30 Jenkin, M. E., Rossi, M. J., Troe, J., and Subcommittee, I.: Evaluated kinetic and  
31 photochemical data for atmospheric chemistry: Volume II - gas phase reactions of organic  
32 species, *Atmos. Chem. Phys.*, 6, 3625-4055, 10.5194/acp-6-3625-2006, 2006.
- 33 Berndt, T., Jokinen, T., Mauldin, R. L., Petaja, T., Herrmann, H., Junninen, H., Paasonen, P.,  
34 Worsnop, D. R., and Sipila, M.: Gas-Phase Ozonolysis of Selected Olefins: The Yield of  
35 Stabilized Criegee Intermediate and the Reactivity toward SO<sub>2</sub>, *J. Phys. Chem. Lett.*, 3, 2892-  
36 2896, 10.1021/jz301158u, 2012.
- 37 Berndt, T., Jokinen, T., Sipilä, M., Mauldin Iii, R. L., Herrmann, H., Stratmann, F., Junninen,  
38 H., and Kulmala, M.: H<sub>2</sub>SO<sub>4</sub> formation from the gas-phase reaction of stabilized Criegee  
39 Intermediates with SO<sub>2</sub>: Influence of water vapour content and temperature, *Atmos Environ*,  
40 89, 603-612, <http://dx.doi.org/10.1016/j.atmosenv.2014.02.062>, 2014a.

1 Berndt, T., Voigtlander, J., Stratmann, F., Junninen, H., Mauldin Iii, R. L., Sipila, M.,  
2 Kulmala, M., and Herrmann, H.: Competing atmospheric reactions of CH<sub>2</sub>OO with SO<sub>2</sub> and  
3 water vapour, *Phys Chem Chem Phys*, 16, 19130-19136, 10.1039/c4cp02345e, 2014b.

4 Berresheim, H., Elste, T., Plass-Dülmer, C., Eisele, F. L., and Tanner, D. J.: Chemical  
5 ionization mass spectrometer for long-term measurements of atmospheric OH and H<sub>2</sub>SO<sub>4</sub>,  
6 *International Journal of Mass Spectrometry*, 202, 91-109, [http://dx.doi.org/10.1016/S1387-](http://dx.doi.org/10.1016/S1387-3806(00)00233-5)  
7 [3806\(00\)00233-5](http://dx.doi.org/10.1016/S1387-3806(00)00233-5), 2000.

8 Birmili, W., Berresheim, H., Plass-Dülmer, C., Elste, T., Gilge, S., Wiedensohler, A., and  
9 Uhrner, U.: The Hohenpeissenberg aerosol formation experiment (HAFEX): a long-term  
10 study including size-resolved aerosol, H<sub>2</sub>SO<sub>4</sub>, OH, and monoterpenes measurements, *Atmos.*  
11 *Chem. Phys.*, 3, 361-376, 10.5194/acp-3-361-2003, 2003.

12 Boy, M., Mogensen, D., Smolander, S., Zhou, L., Nieminen, T., Paasonen, P., Plass-Dülmer,  
13 C., Sipilä, M., Petäjä, T., Mauldin, L., Berresheim, H., and Kulmala, M.: Oxidation of SO<sub>2</sub> by  
14 stabilized Criegee intermediate (sCI) radicals as a crucial source for atmospheric sulfuric acid  
15 concentrations, *Atmos. Chem. Phys.*, 13, 3865-3879, 10.5194/acp-13-3865-2013, 2013.

16 Buras, Z. J., Elsamra, R. M., Jalan, A., Middaugh, J. E., and Green, W. H.: Direct kinetic  
17 measurements of reactions between the simplest Criegee intermediate CH<sub>2</sub>OO and alkenes, *J*  
18 *Phys Chem A*, 118, 1997-2006, 10.1021/jp4118985, 2014.

19 Chao, W., Hsieh, J.-T., Chang, C.-H., and Lin, J. J.-M.: Direct kinetic measurement of the  
20 reaction of the simplest Criegee intermediate with water vapor, *Science*,  
21 10.1126/science.1261549, 2015.

22 Chen, L., Wang, W., Wang, W., Liu, Y., Liu, F., Liu, N., and Wang, B.: Water-catalyzed  
23 decomposition of the simplest Criegee intermediate CH<sub>2</sub>OO, *Theoretical Chemistry*  
24 *Accounts*, 135, 1-13, 10.1007/s00214-016-1894-9, 2016.

25 Chhantyal-Pun, R., Davey, A., Shallcross, D. E., Percival, C. J., and Orr-Ewing, A. J.: A  
26 kinetic study of the CH<sub>2</sub>OO Criegee intermediate self-reaction, reaction with SO<sub>2</sub> and  
27 unimolecular reaction using cavity ring-down spectroscopy, *Phys Chem Chem Phys*,  
28 10.1039/c4cp04198d, 2015.

29 Criegee, R.: Mechanism of Ozonolysis, *Angew. Chem.-Int. Edit. Engl.*, 14, 745-752,  
30 10.1002/anie.197507451, 1975.

31 Di Carlo, P., Brune, W. H., Martinez, M., Harder, H., Leshner, R., Ren, X. R., Thornberry, T.,  
32 Carroll, M. A., Young, V., Shepson, P. B., Riener, D., Apel, E., and Campbell, C.: Missing  
33 OH reactivity in a forest: Evidence for unknown reactive biogenic VOCs, *Science*, 304, 722-  
34 725, 10.1126/science.1094392, 2004.

35 Donahue, N. M., Drozd, G. T., Epstein, S. A., Presto, A. A., and Kroll, J. H.: Adventures in  
36 ozoneland: down the rabbit-hole, *Phys Chem Chem Phys*, 13, 10848-10857,  
37 10.1039/c0cp02564j, 2011.

38 Drozd, G. T., and Donahue, N. M.: Pressure Dependence of Stabilized Criegee Intermediate  
39 Formation from a Sequence of Alkenes, *J Phys Chem A*, 115, 4381-4387,  
40 10.1021/jp2001089, 2011.

41 Drozd, G. T., Kroll, J., and Donahue, N. M.: 2,3-Dimethyl-2-butene (TME) Ozonolysis:  
42 Pressure Dependence of Stabilized Criegee Intermediates and Evidence of Stabilized Vinyl  
43 Hydroperoxides, *J Phys Chem A*, 115, 161-166, 10.1021/jp108773d, 2011.

1 Duhl, T. R., Helmig, D., and Guenther, A.: Sesquiterpene emissions from vegetation: a  
2 review, *Biogeosciences*, 5, 761-777, 10.5194/bg-5-761-2008, 2008.

3 Edwards, P. M., Evans, M. J., Furneaux, K. L., Hopkins, J., Ingham, T., Jones, C., Lee, J. D.,  
4 Lewis, A. C., Moller, S. J., Stone, D., Whalley, L. K., and Heard, D. E.: OH reactivity in a  
5 South East Asian tropical rainforest during the Oxidant and Particle Photochemical Processes  
6 (OP3) project, *Atmos. Chem. Phys.*, 13, 9497-9514, 10.5194/acp-13-9497-2013, 2013.

7 Fang, Y., Liu, F., Barber, V. P., Klippenstein, S. J., McCoy, A. B., and Lester, M. I.:  
8 Communication: Real time observation of unimolecular decay of Criegee intermediates to  
9 OH radical products, *The Journal of Chemical Physics*, 144, 061102,  
10 doi:<http://dx.doi.org/10.1063/1.4941768>, 2016a.

11 Fang, Y., Liu, F., Klippenstein, S. J., and Lester, M. I.: Direct observation of unimolecular  
12 decay of CH<sub>3</sub>CH<sub>2</sub>CHOO Criegee intermediates to OH radical products, *The Journal of*  
13 *Chemical Physics*, 145, 044312, doi:<http://dx.doi.org/10.1063/1.4958992>, 2016b.

14 Fenske, J. D., Hasson, A. S., Ho, A. W., and Paulson, S. E.: Measurement of Absolute  
15 Unimolecular and Bimolecular Rate Constants for CH<sub>3</sub>CHOO Generated by the trans-2-  
16 Butene Reaction with Ozone in the Gas Phase, *The Journal of Physical Chemistry A*, 104,  
17 9921-9932, 10.1021/jp0016636, 2000a.

18 Fenske, J. D., Kuwata, K. T., Houk, K. N., and Paulson, S. E.: OH Radical Yields from the  
19 Ozone Reaction with Cycloalkenes, *The Journal of Physical Chemistry A*, 104, 7246-7254,  
20 10.1021/jp993611q, 2000b.

21 Foreman, E. S., Kapnas, K. M., and Murray, C.: Reactions between Criegee Intermediates  
22 and the Inorganic Acids HCl and HNO<sub>3</sub>: Kinetics and Atmospheric Implications,  
23 *Angewandte Chemie International Edition*, n/a-n/a, 10.1002/anie.201604662, 2016.

24 Fuchs, H., Tan, Z., Hofzumahaus, A., Broch, S., Dorn, H. P., Holland, F., K nstler, C.,  
25 Gomm, S., Rohrer, F., Schrade, S., Tillmann, R., and Wahner, A.: Investigation of potential  
26 interferences in the detection of atmospheric ROx radicals by laser-induced fluorescence  
27 under dark conditions, *Atmos. Meas. Tech.*, 9, 1431-1447, 10.5194/amt-9-1431-2016, 2016.

28 Geyer, A., B chmann, K., Hofzumahaus, A., Holland, F., Konrad, S., Kl pfel, T., P tz, H.-  
29 W., Perner, D., Mihelcic, D., Sch fer, H.-J., Volz-Thomas, A., and Platt, U.: Nighttime  
30 formation of peroxy and hydroxyl radicals during the BERLIOZ campaign: Observations and  
31 modeling studies, *Journal of Geophysical Research: Atmospheres*, 108, 8249,  
32 10.1029/2001jd000656, 2003.

33 Gilge, S., Plass-D lmer, C., Fricke, W., Kaiser, A., Ries, L., Buchmann, B., and Steinbacher,  
34 M.: Ozone, carbon monoxide and nitrogen oxides time series at four alpine GAW mountain  
35 stations in central Europe, *Atmos. Chem. Phys.*, 10, 12295-12316, 10.5194/acp-10-12295-  
36 2010, 2010.

37 Griffith, S. M., Hansen, R. F., Dusanter, S., Stevens, P. S., Alaghmand, M., Bertman, S. B.,  
38 Carroll, M. A., Erickson, M., Galloway, M., Grossberg, N., Hottle, J., Hou, J., Jobson, B. T.,  
39 Kammrath, A., Keutsch, F. N., Lefer, B. L., Mielke, L. H., O'Brien, A., Shepson, P. B.,  
40 Thurlow, M., Wallace, W., Zhang, N., and Zhou, X. L.: OH and HO<sub>2</sub> radical  
41 chemistry during PROPHET 2008 and CABINEX 2009 – Part 1: Measurements and  
42 model comparison, *Atmos. Chem. Phys.*, 13, 5403-5423, 10.5194/acp-13-5403-2013, 2013.

1 Griffith, S. M., Hansen, R. F., Dusanter, S., Michoud, V., Gilman, J. B., Kuster, W. C.,  
2 Veres, P. R., Graus, M., de Gouw, J. A., Roberts, J., Young, C., Washenfelder, R., Brown, S.  
3 S., Thalman, R., Waxman, E., Volkamer, R., Tsai, C., Stutz, J., Flynn, J. H., Grossberg, N.,  
4 Lefer, B., Alvarez, S. L., Rappenglueck, B., Mielke, L. H., Osthoff, H. D., and Stevens, P. S.:  
5 Measurements of hydroxyl and hydroperoxy radicals during CalNex-LA: Model comparisons  
6 and radical budgets, *Journal of Geophysical Research: Atmospheres*, n/a-n/a,  
7 10.1002/2015JD024358, 2016.

8 Guenther, A. B., Zimmerman, P. R., Harley, P. C., Monson, R. K., and Fall, R.: Isoprene and  
9 monoterpene emission rate variability: Model evaluations and sensitivity analyses, *Journal of*  
10 *Geophysical Research: Atmospheres*, 98, 12609-12617, 10.1029/93jd00527, 1993.

11 Hakola, H., Tarvainen, V., Laurila, T., Hiltunen, V., Hellén, H., and Keronen, P.: Seasonal  
12 variation of VOC concentrations above a boreal coniferous forest, *Atmos Environ*, 37, 1623-  
13 1634, [http://dx.doi.org/10.1016/S1352-2310\(03\)00014-1](http://dx.doi.org/10.1016/S1352-2310(03)00014-1), 2003.

14 Handisides, G. M., Plass-Dülmer, C., Gilge, S., Bingemer, H., and Berresheim, H.:  
15 Hohenpeissenberg Photochemical Experiment (HOPE 2000): Measurements and  
16 photostationary state calculations of OH and peroxy radicals, *Atmos. Chem. Phys.*, 3, 1565-  
17 1588, 10.5194/acp-3-1565-2003, 2003.

18 Harrison, R. M., Yin, J., Tilling, R. M., Cai, X., Seakins, P. W., Hopkins, J. R., Lansley, D.  
19 L., Lewis, A. C., Hunter, M. C., Heard, D. E., Carpenter, L. J., Creasey, D. J., Lee, J. D.,  
20 Pilling, M. J., Carslaw, N., Emmerson, K. M., Redington, A., Derwent, R. G., Ryall, D.,  
21 Mills, G., and Penkett, S. A.: Measurement and modelling of air pollution and atmospheric  
22 chemistry in the U.K. West Midlands conurbation: Overview of the PUMA Consortium  
23 project, *Sci. Total Environ.*, 360, 5-25, <http://dx.doi.org/10.1016/j.scitotenv.2005.08.053>,  
24 2006.

25 Hasson, A. S., Ho, A. W., Kuwata, K. T., and Paulson, S. E.: Production of stabilized Criegee  
26 intermediates and peroxides in the gas phase ozonolysis of alkenes: 2. Asymmetric and  
27 biogenic alkenes, *Journal of Geophysical Research: Atmospheres*, 106, 34143-34153,  
28 10.1029/2001jd000598, 2001.

29 Heard, D. E., Carpenter, L. J., Creasey, D. J., Hopkins, J. R., Lee, J. D., Lewis, A. C., Pilling,  
30 M. J., Seakins, P. W., Carslaw, N., and Emmerson, K. M.: High levels of the hydroxyl radical  
31 in the winter urban troposphere, *Geophys Res Lett*, 31, L18112, 10.1029/2004gl020544,  
32 2004.

33 Hens, K., Novelli, A., Martinez, M., Auld, J., Axinte, R., Bohn, B., Fischer, H., Keronen, P.,  
34 Kubistin, D., Nölscher, A. C., Oswald, R., Paasonen, P., Petäjä, T., Regelin, E., Sander, R.,  
35 Sinha, V., Sipilä, M., Taraborrelli, D., Tatum Ernest, C., Williams, J., Lelieveld, J., and  
36 Harder, H.: Observation and modelling of HOx radicals in a boreal forest, *Atmos. Chem.*  
37 *Phys.*, 14, 8723-8747, 10.5194/acp-14-8723-2014, 2014.

38 Hoerger, C. C., Werner, A., Plass-Duelmer, C., Reimann, S., Eckart, E., Steinbrecher, R.,  
39 Aalto, J., Arduini, J., Bonnaire, N., Cape, J. N., Colomb, A., Connolly, R., Diskova, J.,  
40 Dumitrean, P., Ehlers, C., Gros, V., Hakola, H., Hill, M., Hopkins, J. R., Jäger, J., Junek, R.,  
41 Kajos, M. K., Klemp, D., Leuchner, M., Lewis, A. C., Locoge, N., Maione, M., Martin, D.,  
42 Michl, K., Nemitz, E., O'Doherty, S., Pérez Ballesta, P., Ruuskanen, T. M., Sauvage, S.,  
43 Schmidbauer, N., Spain, T. G., Straube, E., Vana, M., Vollmer, M. K., Wegener, R., and  
44 Wenger, A.: ACTRIS non-methane hydrocarbon intercomparison experiment in Europe to



1 support WMO-GAW and EMEP observation networks, Atmos. Meas. Tech. Discuss., 7,  
2 10423-10485, 10.5194/amtd-7-10423-2014, 2014.

3 Horie, O., Neeb, P., and Moortgat, G. K.: The reactions of the Criegee intermediate  
4  $\text{CH}_3\text{CHOO}$  in the gas-phase ozonolysis of 2-butene isomers, Int J Chem Kinet, 29, 461-468,  
5 10.1002/(sici)1097-4601(1997)29:6<461::aid-kin8>3.0.co;2-s, 1997.

6 Horie, O., Schäfer, C., and Moortgat, G. K.: High reactivity of hexafluoroacetone toward  
7 criegee intermediates in the gas-phase ozonolysis of simple alkenes, Int J Chem Kinet, 31,  
8 261-269, 10.1002/(sici)1097-4601(1999)31:4<261::aid-kin3>3.0.co;2-z, 1999.

9 Huang, H.-L., Chao, W., and Lin, J. J.-M.: Kinetics of a Criegee intermediate that would  
10 survive high humidity and may oxidize atmospheric  $\text{SO}_2$ , Proceedings of the National  
11 Academy of Sciences, 10.1073/pnas.1513149112, 2015.

12 Jiang, L., Xu, Y.-s., and Ding, A.-z.: Reaction of Stabilized Criegee Intermediates from  
13 Ozonolysis of Limonene with Sulfur Dioxide: Ab Initio and DFT Study, The Journal of  
14 Physical Chemistry A, 114, 12452-12461, 10.1021/jp107783z, 2010.

15 Johnson, D., and Marston, G.: The gas-phase ozonolysis of unsaturated volatile organic  
16 compounds in the troposphere, Chemical Society Reviews, 37, 699-716, 2008.

17 Junninen, H., Lauri, A., Keronen, P., Aalto, P., Hiltunen, V., Hari, P., and Kulmala, M.:  
18 Smart-SMEAR: on-line data exploration and visualization tool for SMEAR stations, Boreal  
19 Env. Res., 14, 447-457, 2009.

20 Kidwell, N. M., Li, H., Wang, X., Bowman, J. M., and Lester, M. I.: Unimolecular  
21 dissociation dynamics of vibrationally activated  $\text{CH}_3\text{CHOO}$  Criegee intermediates to OH  
22 radical products, Nat Chem, advance online publication, 10.1038/nchem.2488  
23 [http://www.nature.com/nchem/journal/vaop/ncurrent/abs/nchem.2488.html#supplementary-](http://www.nature.com/nchem/journal/vaop/ncurrent/abs/nchem.2488.html#supplementary-information)  
24 [information](http://www.nature.com/nchem/journal/vaop/ncurrent/abs/nchem.2488.html#supplementary-information), 2016.

25 Kroll, J. H., Sahay, S. R., Anderson, J. G., Demerjian, K. L., and Donahue, N. M.:  
26 Mechanism of HOx Formation in the Gas-Phase Ozone-Alkene Reaction. 2. Prompt versus  
27 Thermal Dissociation of Carbonyl Oxides to Form OH, The Journal of Physical Chemistry A,  
28 105, 4446-4457, 10.1021/jp004136v, 2001.

29 Kroll, J. H., Donahue, N. M., Cee, V. J., Demerjian, K. L., and Anderson, J. G.: Gas-Phase  
30 Ozonolysis of Alkenes: Formation of OH from Anti Carbonyl Oxides, J Am Chem Soc, 124,  
31 8518-8519, 10.1021/ja0266060, 2002.

32 Kulmala, M., Maso, M. D., Mäkelä, J. M., Pirjola, L., Väkevä, M., Aalto, P.,  
33 Mikkiläinen, P., Hämeri, K., and O'Dowd, C. D.: On the formation, growth and  
34 composition of nucleation mode particles, Tellus B, 53, 479-490, 10.1034/j.1600-  
35 0889.2001.530411.x, 2001.

36 Kurtén, T., Lane, J. R., Jørgensen, S., and Kjaergaard, H. G.: A Computational Study of the  
37 Oxidation of  $\text{SO}_2$  to  $\text{SO}_3$  by Gas-Phase Organic Oxidants, The Journal of Physical Chemistry  
38 A, 115, 8669-8681, 10.1021/jp203907d, 2011.

39 Kuwata, K. T., Hermes, M. R., Carlson, M. J., and Zogg, C. K.: Computational studies of the  
40 isomerization and hydration reactions of acetaldehyde oxide and methyl vinyl carbonyl oxide,  
41 J Phys Chem A, 114, 9192-9204, 10.1021/jp105358v, 2010.

1 Lee, Y.-P.: Perspective: Spectroscopy and kinetics of small gaseous Criegee intermediates,  
2 The Journal of Chemical Physics, 143, 020901, doi:<http://dx.doi.org/10.1063/1.4923165>,  
3 2015.

4 Lewis, T. R., Blitz, M., Heard, D. E., and Seakins, P.: Direct evidence for a substantive  
5 reaction between the C1 Criegee radical, CH<sub>2</sub>OO, and the water vapour dimer, Phys Chem  
6 Chem Phys, 10.1039/c4cp04750h, 2015.

7 Lin, L.-C., Chang, H.-T., Chang, C.-H., Chao, W., Smith, M. C., Chang, C.-H., Jr-Min Lin,  
8 J., and Takahashi, K.: Competition between H<sub>2</sub>O and (H<sub>2</sub>O)<sub>2</sub> reactions with  
9 CH<sub>2</sub>OO/CH<sub>3</sub>CHOO, Phys Chem Chem Phys, 18, 4557-4568, 10.1039/C5CP06446E, 2016.

10 Liu, F., Beames, J. M., Green, A. M., and Lester, M. I.: UV spectroscopic characterization of  
11 dimethyl- and ethyl-substituted carbonyl oxides, J Phys Chem A, 118, 2298-2306,  
12 10.1021/jp412726z, 2014a.

13 Liu, Y., Bayes, K. D., and Sander, S. P.: Measuring rate constants for reactions of the  
14 simplest Criegee intermediate (CH<sub>2</sub>OO) by monitoring the OH radical, J Phys Chem A, 118,  
15 741-747, 10.1021/jp407058b, 2014b.

16 Long, B., Bao, J. L., and Truhlar, D. G.: Atmospheric Chemistry of Criegee Intermediates.  
17 Unimolecular Reactions and Reactions with Water, J Am Chem Soc, 10.1021/jacs.6b08655,  
18 2016.

19 Mao, J., Ren, X., Zhang, L., Van Duin, D. M., Cohen, R. C., Park, J. H., Goldstein, A. H.,  
20 Paulot, F., Beaver, M. R., Crounse, J. D., Wennberg, P. O., DiGangi, J. P., Henry, S. B.,  
21 Keutsch, F. N., Park, C., Schade, G. W., Wolfe, G. M., Thornton, J. A., and Brune, W. H.:  
22 Insights into hydroxyl measurements and atmospheric oxidation in a California forest,  
23 Atmos. Chem. Phys., 12, 8009-8020, 10.5194/acp-12-8009-2012, 2012.

24 Martinez, M., Harder, H., Kubistin, D., Rudolf, M., Bozem, H., Eerdekens, G., Fischer, H.,  
25 Klupfel, T., Gurk, C., Konigstedt, R., Parchatka, U., Schiller, C. L., Stickler, A., Williams, J.,  
26 and Lelieveld, J.: Hydroxyl radicals in the tropical troposphere over the Suriname rainforest:  
27 airborne measurements, Atmospheric Chemistry and Physics, 10, 3759-3773, 2010.

28 Mauldin III, R. L., Berndt, T., Sipila, M., Paasonen, P., Petaja, T., Kim, S., Kurten, T.,  
29 Stratmann, F., Kerminen, V. M., and Kulmala, M.: A new atmospherically relevant oxidant  
30 of sulphur dioxide, Nature, 488, 193-196,  
31 [http://www.nature.com/nature/journal/v488/n7410/abs/nature11278.html#supplementary-](http://www.nature.com/nature/journal/v488/n7410/abs/nature11278.html#supplementary-information)  
32 [information](http://www.nature.com/nature/journal/v488/n7410/abs/nature11278.html#supplementary-information), 2012.

33 Newland, M. J., Rickard, A. R., Alam, M. S., Vereecken, L., Munoz, A., Rodenas, M., and  
34 Bloss, W. J.: Kinetics of stabilised Criegee intermediates derived from alkene ozonolysis:  
35 reactions with SO<sub>2</sub>, H<sub>2</sub>O and decomposition under boundary layer conditions, Phys Chem  
36 Chem Phys, 10.1039/c4cp04186k, 2015a.

37 Newland, M. J., Rickard, A. R., Vereecken, L., Muñoz, A., Ródenas, M., and Bloss, W. J.:  
38 Atmospheric isoprene ozonolysis: impacts of stabilised Criegee intermediate reactions with  
39 SO<sub>2</sub>, H<sub>2</sub>O and dimethyl sulfide, Atmos. Chem. Phys., 15, 9521-9536, 10.5194/acp-15-9521-  
40 2015, 2015b.

41 Nguyen, T. L., Peeters, J., and Vereecken, L.: Theoretical study of the gas-phase ozonolysis  
42 of beta-pinene (C(10)H(16)), Phys Chem Chem Phys, 11, 5643-5656, 10.1039/b822984h,  
43 2009a.

1 Nguyen, T. L., Winterhalter, R., Moortgat, G., Kanawati, B., Peeters, J., and Vereecken, L.:  
2 The gas-phase ozonolysis of [small beta]-caryophyllene (C<sub>15</sub>H<sub>24</sub>). Part II: A theoretical  
3 study, *Phys Chem Chem Phys*, 11, 4173-4183, 2009b.

4 Nölscher, A. C., Williams, J., Sinha, V., Custer, T., Song, W., Johnson, A. M., Axinte, R.,  
5 Bozem, H., Fischer, H., Pouvesle, N., Phillips, G., Crowley, J. N., Rantala, P., Rinne, J.,  
6 Kulmala, M., Gonzales, D., Valverde-Canossa, J., Vogel, A., Hoffmann, T., Ouwersloot, H.  
7 G., Vilà-Guerau de Arellano, J., and Lelieveld, J.: Summertime total OH reactivity  
8 measurements from boreal forest during HUMPPA-COPEC 2010, *Atmos. Chem. Phys.*, 12,  
9 8257-8270, 10.5194/acp-12-8257-2012, 2012.

10 Novelli, A., Hens, K., Tatum Ernest, C., Kubistin, D., Regelin, E., Elste, T., Plass-Dülmer,  
11 C., Martinez, M., Lelieveld, J., and Harder, H.: Characterisation of an inlet pre-injector laser-  
12 induced fluorescence instrument for the measurement of atmospheric hydroxyl radicals,  
13 *Atmos. Meas. Tech.*, 7, 3413-3430, 10.5194/amt-7-3413-2014, 2014a.

14 Novelli, A., Vereecken, L., Lelieveld, J., and Harder, H.: Direct observation of OH formation  
15 from stabilised Criegee intermediates, *Phys Chem Chem Phys*, 16, 19941-19951,  
16 10.1039/c4cp02719a, 2014b.

17 Ouyang, B., McLeod, M. W., Jones, R. L., and Bloss, W. J.: NO<sub>3</sub> radical production from the  
18 reaction between the Criegee intermediate CH<sub>2</sub>OO and NO<sub>2</sub>, *Phys Chem Chem Phys*, 15,  
19 17070-17075, 10.1039/c3cp53024h, 2013.

20 Paulson, S. E., and Orlando, J. J.: The reactions of ozone with alkenes: An important source  
21 of HO<sub>x</sub> in the boundary layer, *Geophys Res Lett*, 23, 3727-3730, 10.1029/96gl03477, 1996.

22 Paulson, S. E., Chung, M. Y., and Hasson, A. S.: OH Radical Formation from the Gas-Phase  
23 Reaction of Ozone with Terminal Alkenes and the Relationship between Structure and  
24 Mechanism, *The Journal of Physical Chemistry A*, 103, 8125-8138, 10.1021/jp991995e,  
25 1999.

26 Peeters, J., Boullart, W., Pultau, V., Vandenberg, S., and Vereecken, L.: Structure–Activity  
27 Relationship for the Addition of OH to (Poly)alkenes: Site-Specific and Total Rate  
28 Constants, *The Journal of Physical Chemistry A*, 111, 1618-1631, 10.1021/jp066973o, 2007.

29 Percival, C. J., Welz, O., Eskola, A. J., Savee, J. D., Osborn, D. L., Topping, D. O., Lowe, D.,  
30 Utembe, S. R., Bacak, A., McFiggans, G., Cooke, M. C., Xiao, P., Archibald, A. T., Jenkin,  
31 M. E., Derwent, R. G., Riipinen, I., Mok, D. W., Lee, E. P., Dyke, J. M., Taatjes, C. A., and  
32 Shallcross, D. E.: Regional and global impacts of Criegee intermediates on atmospheric  
33 sulphuric acid concentrations and first steps of aerosol formation, *Faraday Discuss*, 165, 45-  
34 73, 10.1039/c3fd00048f, 2013.

35 Petäjä, T., Mauldin, R. L., Kosciuch, E., McGrath, J., Nieminen, T., Paasonen, P., Boy, M.,  
36 Adamov, A., Kotiaho, T., and Kulmala, M.: Sulfuric acid and OH concentrations in a boreal  
37 forest site, *Atmospheric Chemistry and Physics*, 9, 7435-7448, 2009.

38 Pierce, J. R., Evans, M. J., Scott, C. E., D'Andrea, S. D., Farmer, D. K., Swietlicki, E., and  
39 Spracklen, D. V.: Weak global sensitivity of cloud condensation nuclei and the aerosol  
40 indirect effect to Criegee + SO<sub>2</sub> chemistry, *Atmos. Chem. Phys.*, 13, 3163-3176,  
41 10.5194/acp-13-3163-2013, 2013.

42 Plass-Dülmer, C., Michl, K., Ruf, R., and Berresheim, H.: C<sub>2</sub>–C<sub>8</sub> Hydrocarbon measurement  
43 and quality control procedures at the Global Atmosphere Watch Observatory

1 Hohenpeissenberg, Journal of Chromatography A, 953, 175-197,  
2 [http://dx.doi.org/10.1016/S0021-9673\(02\)00128-0](http://dx.doi.org/10.1016/S0021-9673(02)00128-0), 2002.

3 Rathman, W. C. D., Claxton, T. A., Rickard, A. R., and Marston, G.: A theoretical  
4 investigation of OH formation in the gas-phase ozonolysis of E-but-2-ene and Z-but-2-ene,  
5 Phys Chem Chem Phys, 1, 3981-3985, 10.1039/a903186c, 1999.

6 Ren, X., Harder, H., Martinez, M., Leshner, R. L., Oligier, A., Simpas, J. B., Brune, W. H.,  
7 Schwab, J. J., Demerjian, K. L., He, Y., Zhou, X., and Gao, H.: OH and HO<sub>2</sub> Chemistry in  
8 the urban atmosphere of New York City, Atmos Environ, 37, 3639-3651,  
9 [http://dx.doi.org/10.1016/S1352-2310\(03\)00459-X](http://dx.doi.org/10.1016/S1352-2310(03)00459-X), 2003.

10 Rickard, A. R., Johnson, D., McGill, C. D., and Marston, G.: OH Yields in the Gas-Phase  
11 Reactions of Ozone with Alkenes, The Journal of Physical Chemistry A, 103, 7656-7664,  
12 10.1021/jp9916992, 1999.

13 Ryzhkov, A. B., and Ariya, P. A.: A theoretical study of the reactions of carbonyl oxide with  
14 water in atmosphere: the role of water dimer, Chemical Physics Letters, 367, 423-429,  
15 [http://dx.doi.org/10.1016/S0009-2614\(02\)01685-8](http://dx.doi.org/10.1016/S0009-2614(02)01685-8), 2003.

16 Ryzhkov, A. B., and Ariya, P. A.: A theoretical study of the reactions of parent and  
17 substituted Criegee intermediates with water and the water dimer, Phys Chem Chem Phys, 6,  
18 5042-5050, 10.1039/b408414d, 2004.

19 Sarwar, G., Fahey, K., Kwok, R., Gilliam, R. C., Roselle, S. J., Mathur, R., Xue, J., Yu, J.,  
20 and Carter, W. P. L.: Potential impacts of two SO<sub>2</sub> oxidation pathways on regional sulfate  
21 concentrations: Aqueous-phase oxidation by NO<sub>2</sub> and gas-phase oxidation by Stabilized  
22 Criegee Intermediates, Atmos Environ, 68, 186-197,  
23 <http://dx.doi.org/10.1016/j.atmosenv.2012.11.036>, 2013.

24 Sarwar, G., Simon, H., Fahey, K., Mathur, R., Goliff, W. S., and Stockwell, W. R.: Impact of  
25 sulfur dioxide oxidation by Stabilized Criegee Intermediate on sulfate, Atmos Environ, 85,  
26 204-214, DOI 10.1016/j.atmosenv.2013.12.013, 2014.

27 Shallcross, D. E., Taatjes, C. A., and Percival, C. J.: Criegee intermediates in the indoor  
28 environment: new insights, Indoor Air, n/a-n/a, 10.1111/ina.12102, 2014.

29 Sheps, L., Scully, A. M., and Au, K.: UV absorption probing of the conformer-dependent  
30 reactivity of a Criegee intermediate CH<sub>3</sub>CHOO, Phys Chem Chem Phys,  
31 10.1039/c4cp04408h, 2014.

32 Shillings, A. J. L., Ball, S. M., Barber, M. J., Tennyson, J., and Jones, R. L.: An upper limit  
33 for water dimer absorption in the 750 nm spectral region and a revised water line list, Atmos.  
34 Chem. Phys., 11, 4273-4287, 10.5194/acp-11-4273-2011, 2011.

35 Sinha, V., Williams, J., Crowley, J. N., and Lelieveld, J.: The Comparative Reactivity  
36 Method &ndash; a new tool to measure total OH Reactivity in ambient air, Atmos. Chem.  
37 Phys., 8, 2213-2227, 10.5194/acp-8-2213-2008, 2008.

38 Sipilä, M., Jokinen, T., Berndt, T., Richters, S., Makkonen, R., Donahue, N. M., Mauldin Iii,  
39 R. L., Kurtén, T., Paasonen, P., Sarnela, N., Ehn, M., Junninen, H., Rissanen, M. P.,  
40 Thornton, J., Stratmann, F., Herrmann, H., Worsnop, D. R., Kulmala, M., Kerminen, V. M.,  
41 and Petäjä, T.: Reactivity of stabilized Criegee intermediates (sCIs) from isoprene and  
42 monoterpene ozonolysis toward SO<sub>2</sub> and organic acids, Atmos. Chem. Phys., 14, 12143-  
43 12153, 10.5194/acp-14-12143-2014, 2014.

- 1 Smith, M. C., Chang, C.-H., Chao, W., Lin, L.-C., Takahashi, K., Boering, K. A., and Lin, J.  
2 J.-M.: Strong Negative Temperature Dependence of the Simplest Criegee Intermediate  
3 CH<sub>2</sub>OO Reaction with Water Dimer, *The Journal of Physical Chemistry Letters*, 2708-2713,  
4 10.1021/acs.jpcllett.5b01109, 2015.
- 5 Smith, M. C., Chao, W., Takahashi, K., Boering, K. A., and Lin, J. J.-M.: Unimolecular  
6 Decomposition Rate of the Criegee Intermediate (CH<sub>3</sub>)<sub>2</sub>COO Measured Directly with UV  
7 Absorption Spectroscopy, *The Journal of Physical Chemistry A*, 10.1021/acs.jpca.5b12124,  
8 2016.
- 9 Stone, D., Blitz, M., Daubney, L., Howes, N. U., and Seakins, P.: Kinetics of CH<sub>2</sub>OO  
10 reactions with SO<sub>2</sub>, NO<sub>2</sub>, NO, H<sub>2</sub>O and CH<sub>3</sub>CHO as a function of pressure, *Phys Chem Chem*  
11 *Phys*, 16, 1139-1149, 10.1039/c3cp54391a, 2014.
- 12 Taatjes, C. A., Welz, O., Eskola, A. J., Savee, J. D., Scheer, A. M., Shallcross, D. E.,  
13 Rotavera, B., Lee, E. P., Dyke, J. M., Mok, D. K., Osborn, D. L., and Percival, C. J.: Direct  
14 measurements of conformer-dependent reactivity of the Criegee intermediate CH<sub>3</sub>CHOO,  
15 *Science*, 340, 177-180, 10.1126/science.1234689, 2013.
- 16 Taatjes, C. A., Shallcross, D. E., and Percival, C. J.: Research frontiers in the chemistry of  
17 Criegee intermediates and tropospheric ozonolysis, *Phys Chem Chem Phys*, 16, 1704-1718,  
18 10.1039/c3cp52842a, 2014.
- 19 Tan, Z., Fuchs, H., Lu, K., Bohn, B., Broch, S., Dong, H., Gomm, S., Haeseler, R., He, L.,  
20 Hofzumahaus, A., Holland, F., Li, X., Liu, Y., Lu, S., Rohrer, F., Shao, M., Wang, B., Wang,  
21 M., Wu, Y., Zeng, L., Zhang, Y., Wahner, A., and Zhang, Y.: Radical chemistry at a rural site  
22 (Wangdu) in the North China Plain: Observation and model calculations of OH, HO<sub>2</sub> and  
23 RO<sub>2</sub> radicals, *Atmos. Chem. Phys. Discuss.*, 2016, 1-48, 10.5194/acp-2016-614, 2016.
- 24 Tobias, H. J., and Ziemann, P. J.: Kinetics of the Gas-Phase Reactions of Alcohols,  
25 Aldehydes, Carboxylic Acids, and Water with the C<sub>13</sub> Stabilized Criegee Intermediate  
26 Formed from Ozonolysis of 1-Tetradecene, *The Journal of Physical Chemistry A*, 105, 6129-  
27 6135, 10.1021/jp004631r, 2001.
- 28 Vereecken, L., and Francisco, J. S.: Theoretical studies of atmospheric reaction mechanisms  
29 in the troposphere, *Chemical Society Reviews*, 41, 6259-6293, 10.1039/c2cs35070j, 2012.
- 30 Vereecken, L., Harder, H., and Novelli, A.: The reaction of Criegee intermediates with NO,  
31 RO<sub>2</sub>, and SO<sub>2</sub>, and their fate in the atmosphere, *Phys Chem Chem Phys*, 14, 14682-14695,  
32 10.1039/c2cp42300f, 2012.
- 33 Vereecken, L., Harder, H., and Novelli, A.: The reactions of Criegee intermediates with  
34 alkenes, ozone, and carbonyl oxides, *Phys Chem Chem Phys*, 16, 4039-4049,  
35 10.1039/c3cp54514h, 2014.
- 36 Vereecken, L., Glowacki, D. R., and Pilling, M. J.: Theoretical Chemical Kinetics in  
37 Tropospheric Chemistry: Methodologies and Applications, *Chemical Reviews*,  
38 10.1021/cr500488p, 2015.
- 39 Wayne, R. P.: *Chemistry of Atmosphere*, Oxford University Press: Oxford, 2000.
- 40 Welz, O., Savee, J. D., Osborn, D. L., Vasu, S. S., Percival, C. J., Shallcross, D. E., and  
41 Taatjes, C. A.: Direct Kinetic Measurements of Criegee Intermediate (CH<sub>2</sub>OO) Formed by  
42 Reaction of CH<sub>2</sub>I with O<sub>2</sub>, *Science*, 335, 204-207, 10.1126/science.1213229, 2012.

1 White, J. U.: Long optical paths of large aperture, *J. Opt. Soc. Am.*, 32, 285-288,  
2 10.1364/josa.32.000285, 1942.

3 Williams, J., Crowley, J., Fischer, H., Harder, H., Martinez, M., Petäjä, T., Rinne, J., Bäck, J.,  
4 Boy, M., Dal Maso, M., Hakala, J., Kajos, M., Keronen, P., Rantala, P., Aalto, J., Aaltonen,  
5 H., Paatero, J., Vesala, T., Hakola, H., Levula, J., Pohja, T., Herrmann, F., Auld, J.,  
6 Mesarchaki, E., Song, W., Yassaa, N., Nölscher, A., Johnson, A. M., Custer, T., Sinha, V.,  
7 Thieser, J., Pouvesle, N., Taraborrelli, D., Tang, M. J., Bozem, H., Hosaynali-Beygi, Z.,  
8 Axinte, R., Oswald, R., Novelli, A., Kubistin, D., Hens, K., Javed, U., Trawny, K.,  
9 Breitenberger, C., Hidalgo, P. J., Ebben, C. J., Geiger, F. M., Corrigan, A. L., Russell, L. M.,  
10 Ouwersloot, H. G., Vilà-Guerau de Arellano, J., Ganzeveld, L., Vogel, A., Beck, M., Bayerle,  
11 A., Kampf, C. J., Bertelmann, M., Köllner, F., Hoffmann, T., Valverde, J., González, D.,  
12 Riekkola, M. L., Kulmala, M., and Lelieveld, J.: The summertime Boreal forest field  
13 measurement intensive (HUMPPA-COPEC-2010): an overview of meteorological and  
14 chemical influences, *Atmos. Chem. Phys.*, 11, 10599-10618, 10.5194/acp-11-10599-2011,  
15 2011.

16 Woodward-Massey, R., Cryer, D. R., Whalley, L. K., Ingham, T., Seakins, P. W., Heard, D.  
17 E., and Stimpson, L. M.: Implementation of a chemical background method (OH-CHEM) for  
18 measurements of OH using the Leeds FAGE instrument: Characterisation and observations  
19 from a coastal location. , Abstract A41A-0002 presented at 2015 Fall Meeting, AGU, San  
20 Francisco, Calif., 14-18 Dec, 2015.

21 Yassaa, N., Song, W., Lelieveld, J., Vanhatalo, A., Back, J., and Williams, J.: Diel cycles of  
22 isoprenoids in the emissions of Norway spruce, four Scots pine chemotypes, and in Boreal  
23 forest ambient air during HUMPPA-COPEC-2010, *Atmospheric Chemistry and Physics*, 12,  
24 7215-7229, 10.5194/acp-12-7215-2012, 2012.

25 York, D., Evensen, N. M., Martínez, M. L., and De Basabe Delgado, J.: Unified equations for  
26 the slope, intercept, and standard errors of the best straight line, *American Journal of Physics*,  
27 72, 367-375, doi:<http://dx.doi.org/10.1119/1.1632486>, 2004.

28 Zhang, D., and Zhang, R.: Mechanism of OH Formation from Ozonolysis of Isoprene: A  
29 Quantum-Chemical Study, *J Am Chem Soc*, 124, 2692-2703, 10.1021/ja011518l, 2002.

30 Zhu, C., Kumar, M., Zhong, J., Li, L., Francisco, J. S., and Zeng, X. C.: New Mechanistic  
31 Pathways for Criegee–Water Chemistry at the Air/Water Interface, *J Am Chem Soc*,  
32 10.1021/jacs.6b04338, 2016.

33  
34  
35

1 Table 1. Average concentration (molecule cm<sup>-3</sup>), with 1σ variability, of trace gases relevant for this  
2 study.

Compound	HUMPPA-COPEC 2010	HOPE 2012
SO <sub>2</sub> <sup>a</sup>	(1.4 ± 1.7) x 10 <sup>10</sup>	(2.2 ± 2.3) x 10 <sup>9</sup>
H <sub>2</sub> SO <sub>4</sub> <sup>a</sup>	(2.0 ± 2.0) x 10 <sup>6</sup>	(8.5 ± 8.5) x 10 <sup>5</sup>
OH <sup>a</sup>	(7.0 ± 8.0) x 10 <sup>5</sup>	(1.6 ± 1.6) x 10 <sup>6</sup>
O <sub>3</sub> <sup>a</sup>	(1.1 ± 0.2) x 10 <sup>12</sup>	(1.1 ± 0.3) x 10 <sup>12</sup>
Σ[VOC] <sup>a,b</sup>	(7.3 ± 7.1) x 10 <sup>9</sup>	(9.8 ± 9.0) x 10 <sup>9</sup>
OH Reactivity <sup>c</sup>	9.0 ± 7.6	3.5 ± 3.0
Condensation sink (CS) <sup>c</sup>	(10 ± 4.0) x 10 <sup>-3</sup>	(7.0 ± 3.0) x 10 <sup>-3</sup>

3 a, Units: molecules cm<sup>-3</sup>.

4 b, HUMPPA COPEC 2010: isoprene, (-)/(+) α-pinene, (-)/(+) β-pinene, 3-carene, and  
5 myrcene.

6 HOPE 2012: isoprene, α-pinene, β-pinene, 3-carene, myrcene, limonene, 2-  
7 methylpropene, but-1-ene, sabinene, γ-terpinene, propene, cis-2-butene and ethene.

8 c, Units: s<sup>-1</sup>.

9 1 ppbv = 2.5 x 10<sup>10</sup> molecules cm<sup>-3</sup> at 295K and 1013 hPa.

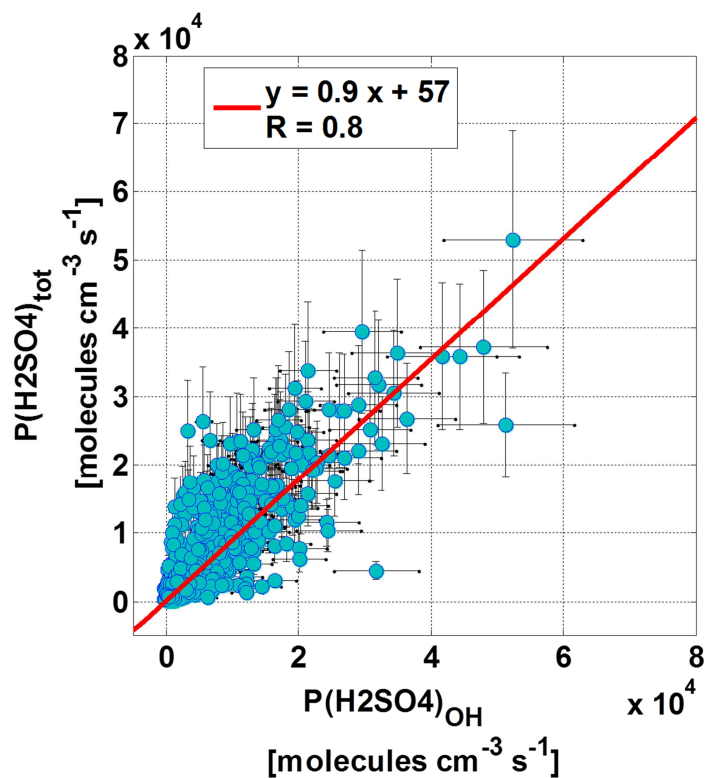
10  
11  
12  
13

1 Table 2. SCI estimates for the HUMPPA-COPEC 2010 and HOPE 2012 campaigns. Average  
 2 concentration (molecule cm<sup>-3</sup>), with 1σ variability.

Approach	HUMPPA-COPEC 2010	HOPE 2012
Missing H <sub>2</sub> SO <sub>4</sub>	(2.3 ± 2.0) x 10 <sup>4</sup> <sup>a</sup>	(2.0 ± 3.0) x 10 <sup>4</sup> <sup>a</sup>
	(1.6 ± 2.0) x 10 <sup>6</sup> <sup>b</sup>	(1.0 ± 3.0) x 10 <sup>6</sup> <sup>b</sup>
Measured unsaturated VOC	(5.0 ± 4.0) x 10 <sup>3</sup>	(7.0 ± 6.0) x 10 <sup>3</sup>
Unexplained OH reactivity	(1.0 ± 1.0) x 10 <sup>5</sup>	(2.0 ± 1.5) x 10 <sup>4</sup>
Unexplained OH production	(2.0 ± 2.0) x 10 <sup>4</sup> <sup>c</sup>	n. a.
	(4.0 ± 4.0) x 10 <sup>5</sup> <sup>d</sup>	n. a.

3 a, k<sub>SCI+SO2</sub> = 3.3 × 10<sup>-11</sup> cm<sup>3</sup> molecule<sup>-1</sup> s<sup>-1</sup>  
 4 b, k<sub>SCI+SO2</sub> = 5.0 × 10<sup>-13</sup> cm<sup>3</sup> molecule<sup>-1</sup> s<sup>-1</sup>  
 5 c,  $P_{OH}^{unexplained}$  = 1.0 x 10<sup>6</sup> molecule cm<sup>-3</sup> s<sup>-1</sup>  
 6 d,  $P_{OH}^{unexplained}$  = 2.0 x 10<sup>7</sup> molecule cm<sup>-3</sup> s<sup>-1</sup>  
 7 1 ppbv = 2.5 x 10<sup>10</sup> molecules cm<sup>-3</sup> at 295K and 1013 hPa.

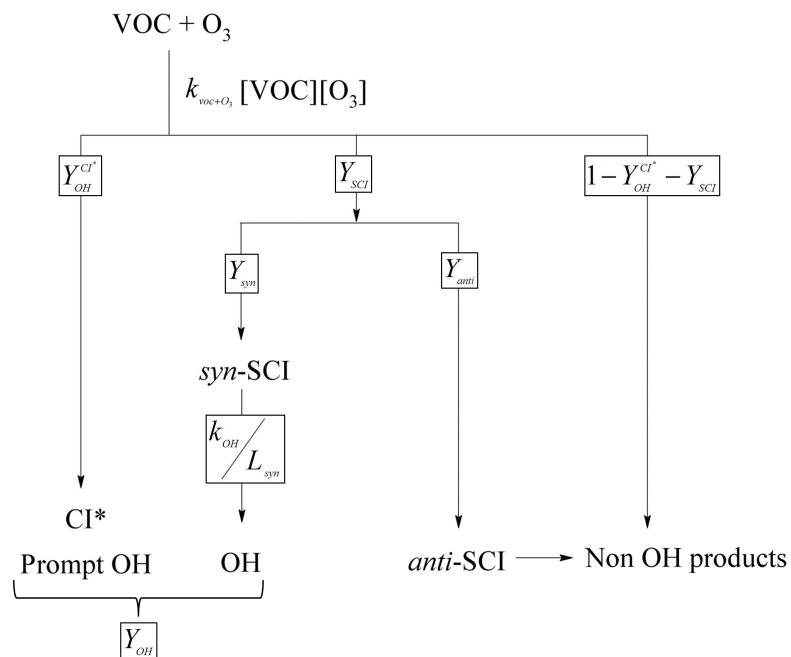




1

2 Figure 1. Total production rate of  $\text{H}_2\text{SO}_4$  ( $P(\text{H}_2\text{SO}_4)_{\text{tot}}$ ) as a function of the production rate of  
 3  $\text{H}_2\text{SO}_4$  from the reaction between OH and  $\text{SO}_2$  during the HOPE 2012 campaign. The linear  
 4 regression, following the method of York et al. (2004), yields a slope of  $0.9 \pm 0.02$  and a  
 5 intercept of  $57 \pm 7$ .

6



1

2 Figure 2. Schematic representation of the formation of OH from the ozonolysis of unsaturated

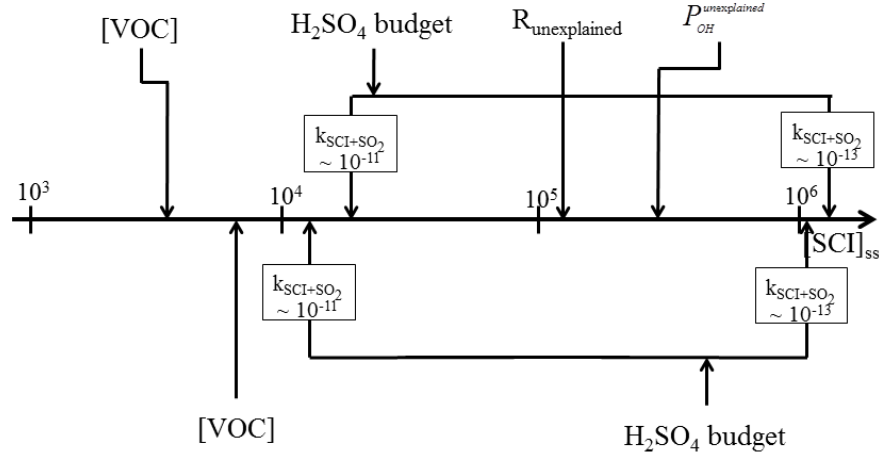
3 VOC.

4

5

6

Boreal Forest (HUMPPA-COPEC 2010)



(Rural Europe)HOPE 2012

Figure 3. Schematic overview of the estimated steady state concentration of SCI ( $[SCI]_{ss}$ , molecules  $\text{cm}^{-3}$ ) observed during the HUMPPA-COPEC 2010 and HOPE 2012 campaigns. For both campaigns the SCI estimate is based on the unsaturated VOC concentration measured,  $[VOC]$ , and the  $\text{H}_2\text{SO}_4$  budget using different SCI+ $\text{SO}_2$  rate coefficients ( $k_{\text{SCI}+\text{SO}_2}$  in  $\text{cm}^3 \text{ molecule}^{-1} \text{ s}^{-1}$ ). In addition, during the HUMPPA-COPEC campaign SCI can be calculated from the unexplained OH reactivity,  $R_{\text{unexplained}}$ , and unexplained OH production,  $P_{\text{unexplained}}^{\text{OH}}$ . See main text for more details (Section 3).

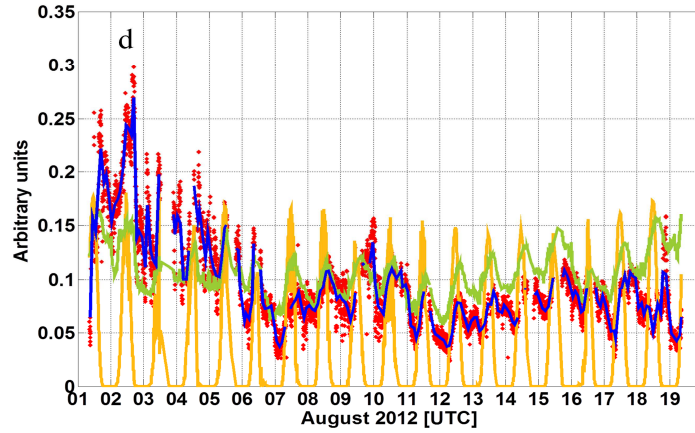
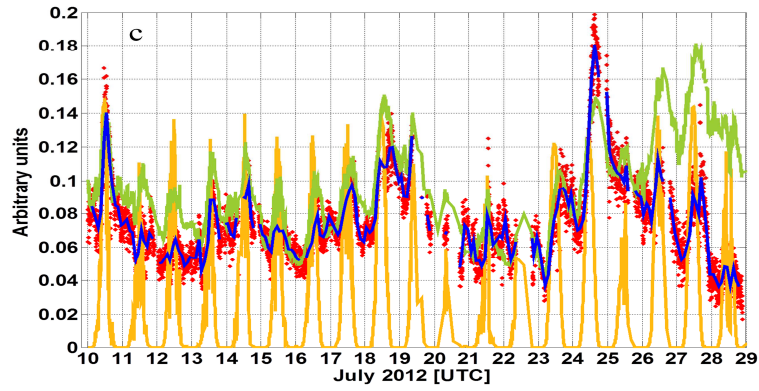
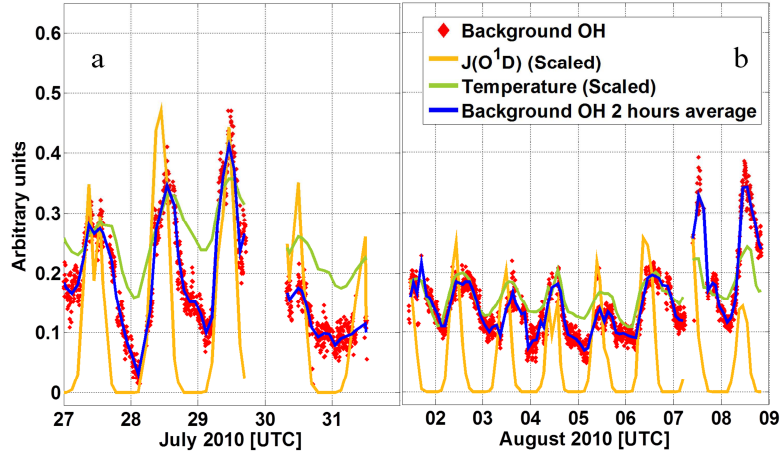
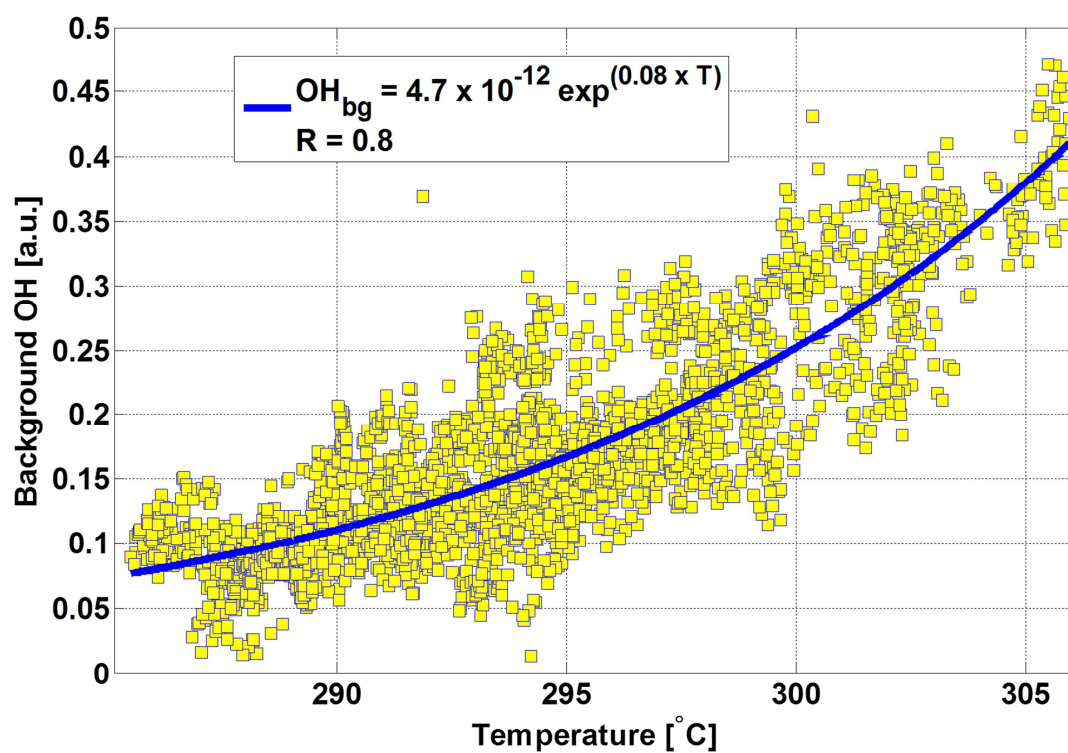


Figure 4. Background OH (red diamonds) measured during the HUMPPA-COPEC 2010 (a, ground and b, tower) and the HOPE 2012 (c, July and d, August) campaigns together with scaled J(O<sup>1</sup>D), multiplied by  $4.0 \times 10^4$  and  $4.0 \times 10^3$  for HUMPPA-COPEC 2010 and HOPE 2012, respectively (orange), and scaled temperature divided by 90 and 160 K for HUMPPA-COPEC 2010 and HOPE 2012, respectively (green).



1

2 Figure 5. Background OH as a function of the temperature during the HUMPPA-COPEC  
 3 2010 campaign.

4

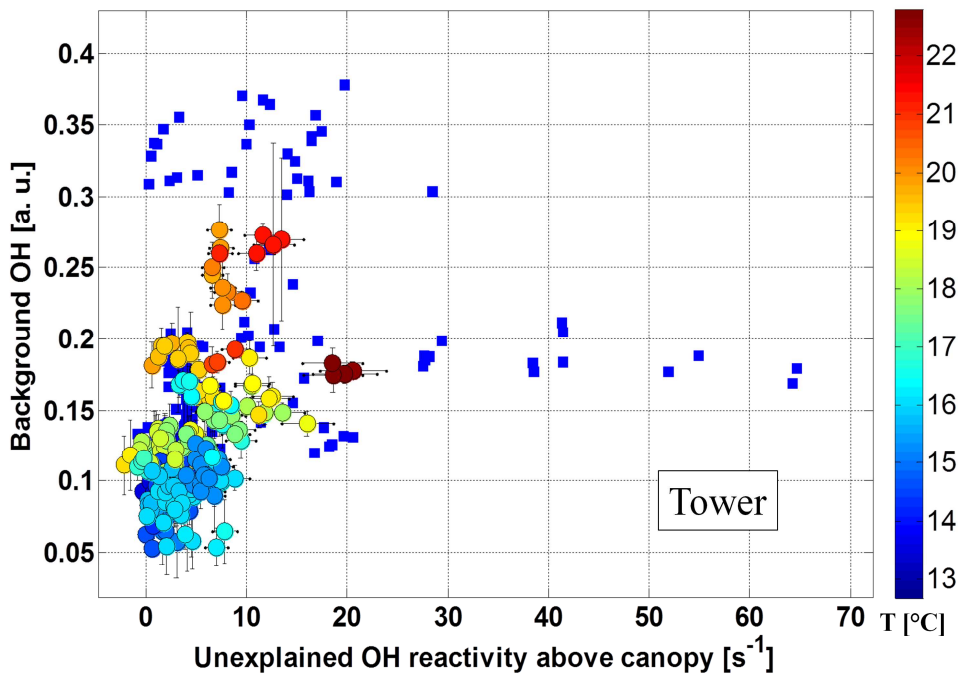
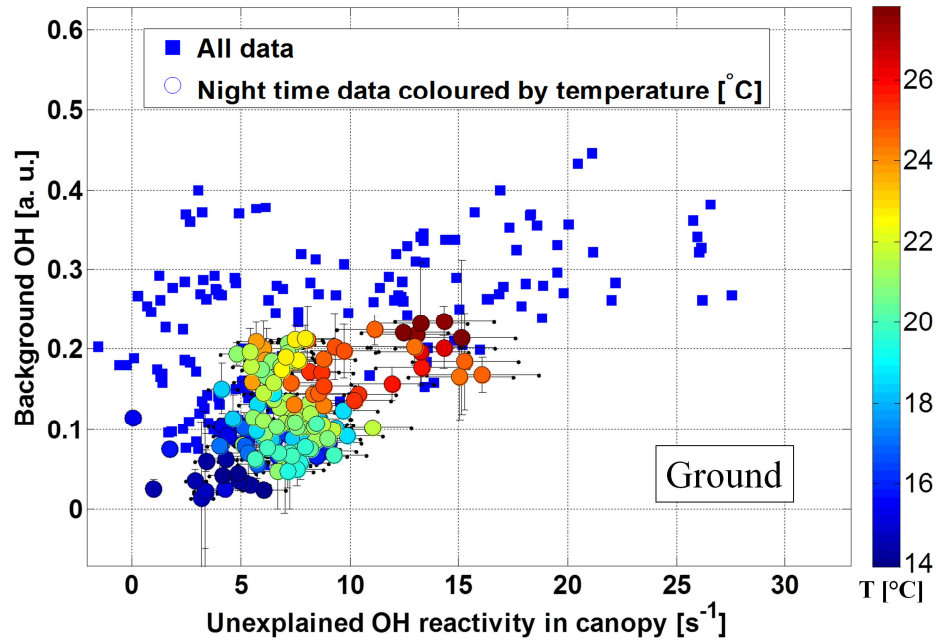
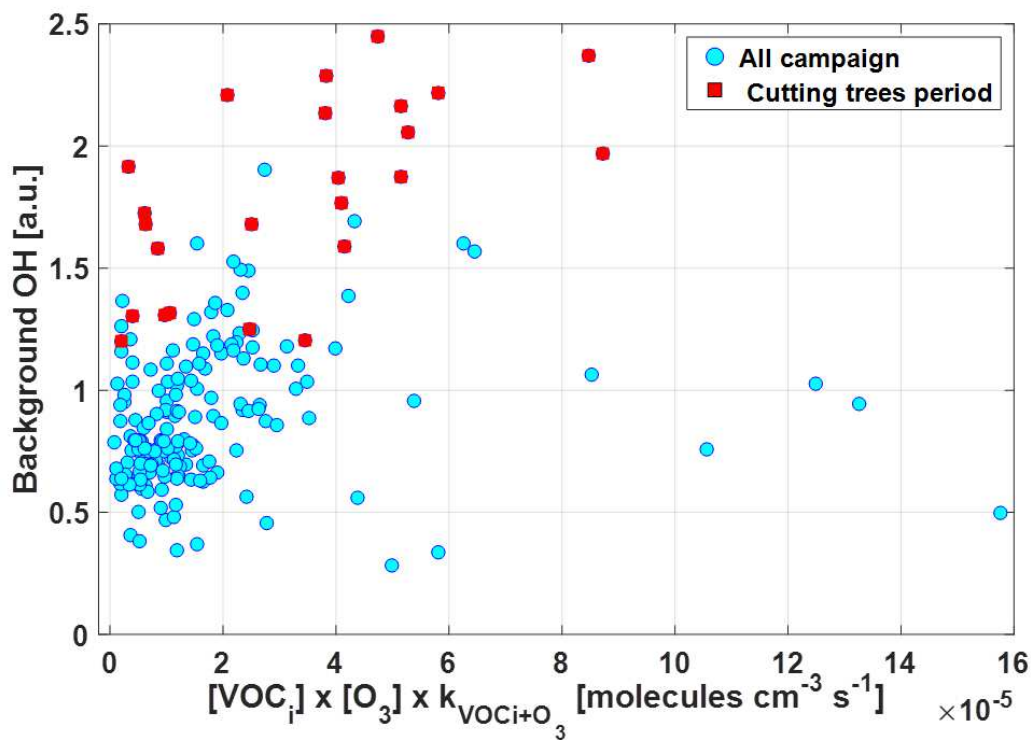


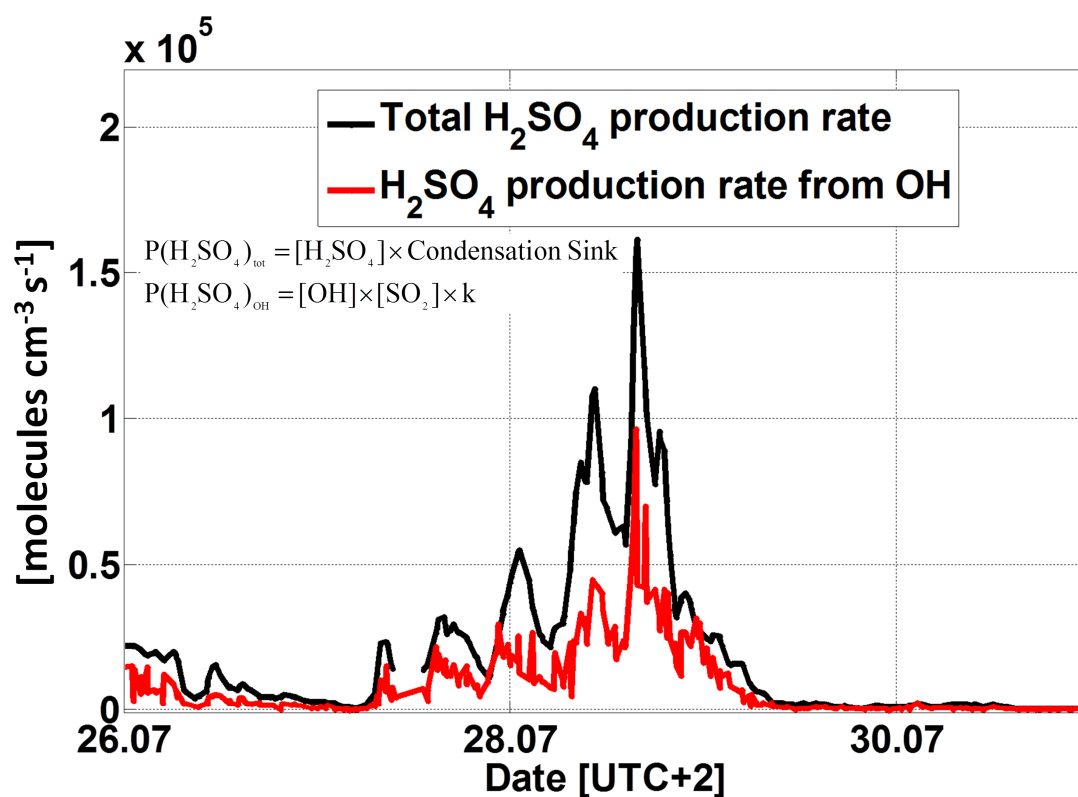
Figure 6. Background OH as a function of unexplained OH reactivity for ground and tower period measurements during the HUMPPA-COPEC 2010 campaign. Squares represent the daytime data, bullets represent night time data and are coloured accordingly to temperature (right legend).



1

2 Figure 7. Background OH as a function of the sum of the product of the measured  
 3 unsaturated VOC-ozone turn-over (Table SI-1), during the HOPE 2012 campaign. The blue  
 4 points refer to the entire field campaign excluding tree cutting, which occurred between 1<sup>st</sup>  
 5 and 3<sup>rd</sup> of August 2012, described by the red squares.

6

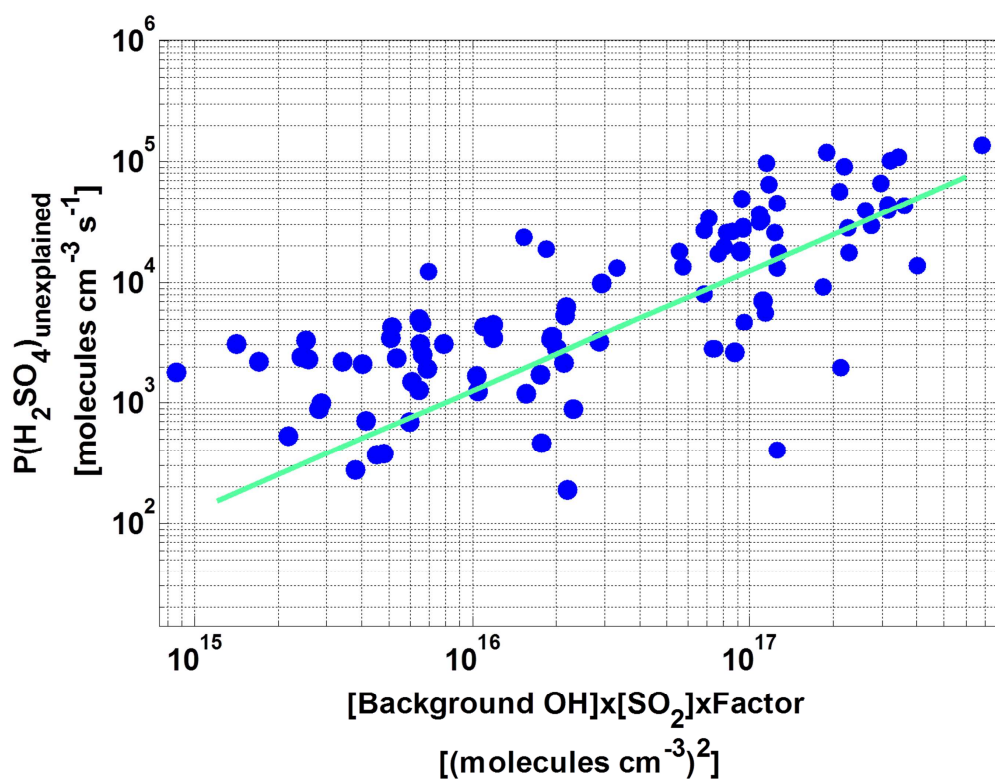


1

2 Figure 8. Comparison of the total  $\text{H}_2\text{SO}_4$  production rate (black line), calculated from the  
 3 measured  $\text{H}_2\text{SO}_4$ , and the production rate of  $\text{H}_2\text{SO}_4$  (red line) involving only the oxidation  
 4 process of  $\text{SO}_2$  by OH for the ground measurements during the HUMPPA-COPEC 2010  
 5 campaign.

6





1

2 Figure 9. The production rate of  $\text{H}_2\text{SO}_4$  unaccounted for by the oxidation of  $\text{SO}_2$  by OH as a  
 3 function of the  $\text{OH}_{\text{bg}}$  multiplied by  $\text{SO}_2$  concentration during the ground measurements of the  
 4 HUMPPA-COPEC 2010 campaign.  $\text{OH}_{\text{bg}}$  is expressed in molecules  $\text{cm}^{-3}$  equivalents of OH.

5

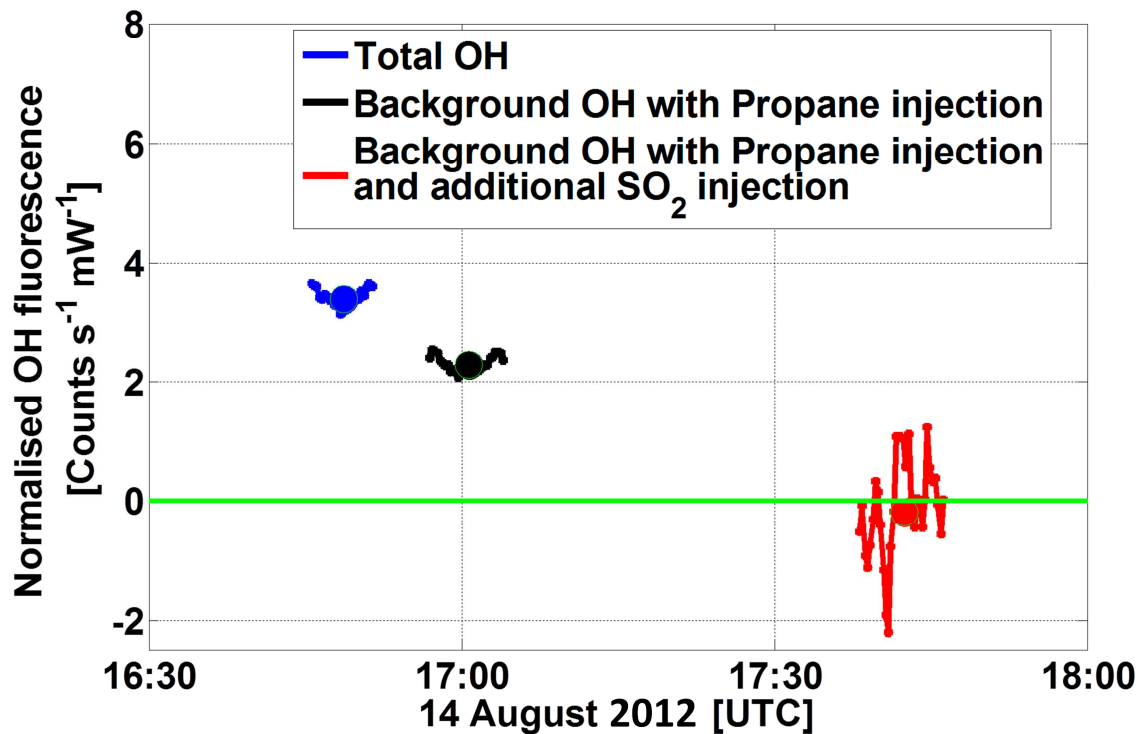
6

7

8

9

10



1  
2 Figure 10. SO<sub>2</sub> injection test within IPI during the HOPE 2012 campaign. The blue data  
3 points represent the total OH measured when no injection is performed. The black data points  
4 represent the background OH measured while injecting propane ( $2.5 \times 10^{15}$  molecules cm<sup>-3</sup>)  
5 scavenging > 90 % of ambient OH. The red signal is the background OH observed when SO<sub>2</sub>  
6 ( $1.0 \times 10^{13}$  molecules cm<sup>-3</sup>) is injected in addition to propane.

7